Computing Fuzzy Trajectories for Nonlinear Dynamic Systems

D. Andrei Măceş[1] and Mark A. Stadtherr[2]

Department of Chemical and Biomolecular Engineering
University of Notre Dame, Notre Dame, IN 46556, USA

May 15, 2012
(revised, November 19, 2012)

[1]E-mail: dmaces@nd.edu
[2]Author to whom all correspondence should be addressed. E-mail: markst@nd.edu

Abstract

One approach for representing uncertainty is the use of fuzzy sets or fuzzy numbers. A new approach is described for the solution of nonlinear dynamic systems with parameters and/or initial states that are uncertain and represented by fuzzy sets or fuzzy numbers. Unlike current methods, which address this problem through the use of sampling techniques and do not account rigorously for the effect of the uncertain quantities, the new approach is not based on sampling and provides mathematically and computationally rigorous results. This is achieved through the use of explicit analytic representations (Taylor models) of state variable bounds in terms of the uncertain quantities. Examples are given that demonstrate the use of this new approach and its computational performance.

Keywords: Uncertainty; Fuzzy sets; Fuzzy numbers; Nonlinear dynamic systems; Interval analysis; Dynamic simulation

1 Introduction

In the context of engineering and science, nonlinear dynamic models typically involve uncertain quantities. For example, in an initial value problem (IVP) described by a system of ordinary differential equations (ODEs), the initial conditions may be uncertain, and there may be uncertain parameters in the ODE model. Determining the effect of such uncertainties on the model outputs is clearly an important issue. To address this problem requires first that an appropriate representation of the uncertain quantities be chosen, and then that these be propagated through the nonlinear ODE model to determine the corresponding uncertainties in the model outputs.

There are a number of approaches that can be used to represent uncertainty. A common approach is to treat an uncertain quantity as a random variable described by some probability distribution. However, the true probability distribution may itself be uncertain. This gives rise to the concept of a probability distribution variable, as described by Li & Hyman (2004), which is typically characterized by a probability box (p-box) (Ferson et al., 1996; Williamson & Downs, 1990) that provides bounds on the probability distribution function. However, many types of uncertainty arise from lack of knowledge, not from randomness, and so may not be appropriately represented through the use of probabilities. In this case, one simple approach is to treat an uncertain quantity as an interval. This requires only knowledge of an upper and lower bound on the uncertainty, and implies nothing about the distribution of the uncertainty. If there is more insight into the nature of the uncertainty, then it might be represented using a fuzzy set (Zadeh, 1965) or a fuzzy number (a particular type of fuzzy set) (Nahmias, 1977; Dubois & Prade, 1980; Kaufmann & Gupta, 1985; Hanss, 2005). Fuzzy sets can be viewed as representing *possibilities*, not probabilities, and form the basis for a theory of possibility (Zadeh, 1978) that is a counterpart to the traditional theory of probability. The relationships between possibilities and probabilities have been well explored (e.g., Dubois & Prade, 1982; Klir & Parviz, 1992; Gupta, 1993; Dubois et al., 2004), with a basis in Zadeh's (1978) possibility/probability consistency principle. This states that something must be possible before it can be probable. Thus, one simple interpretation of possibility is as an upper bound on probability. A fuzzy number can be interpreted as a nested set of intervals, with each successively smaller interval representing a range that is "more possible" than the larger one before it.

Hanss (2005) provides several examples of the use of fuzzy numbers to represent uncertainties in engineering problems involving linear and nonlinear ODE and PDE models. The formulation and solution of such "fuzzy-parameterized" models is a subdomain of fuzzy set theory that has received relatively little attention, with much more work having been focused on the use of fuzzy logic and reasoning methods. For example, just within the field of chemical engineering, there have been many applications of fuzzy logic and reasoning, in process control (e.g., Gromov et al., 1995; Chen et al., 2001; Andujar & Bravo, 2005; Chen & Chang, 2006; Sanjuan et al., 2006; Zhang et al., 2006; Kaucsár et al., 2007), safety and reliability analysis (e.g., Yu & Lee, 1991; Takeda et al., 1994; Guimarães & Lapa, 2004; Meel & Seider, 2006; Yong et al., 2007; Hassana et al., 2009), knowledge processing (e.g., Arva & Csukas, 1987; Vrba, 1991; Hanratty & Joseph, 1992; Hanratty et al., 1992; Dohnal et al., 1994; Gromov et al., 1996; Johansen & Foss, 1997; Schmitz & Aldrich, 1998; Tsekouras et al., 2002; Claudel et al., 2003; Stephane & Marc, 2008), and other areas.

In this paper, we will focus on the use of fuzzy sets and fuzzy numbers to represent uncertainties in nonlinear dynamic models, and consider how to compute the resulting fuzzy trajectories in a verified way. For propagation of fuzzy uncertainties in dynamic models, a typical approach is to solve the underlying ODE problem multiple times using prescribed and/or arbitrary samples of the uncertainty quantities. For example, this is the basis of the "transformation method" of Hanss (2002, 2005). In general, however, this approach is not rigorous and may underestimate the true effect of an uncertain quantity on the model outputs, as discussed in more detail below. We will describe here a much different strategy for the propagation of fuzzy uncertainties in dynamic models. This approach is not based on sampling, and provides mathematically and computationally rigorous results in all cases. Our method is based on the use of techniques (Lin & Stadtherr, 2007) developed for the verified solution of parametric ODE systems. These techniques provide explicit analytic representations (Taylor models) of the state variables, from which rigorous interval bounds on the state variables can be obtained. We explore here how to extend these techniques to provide rigorous fuzzy set bounds on the state variables in fuzzy-parameterized, nonlinear dynamic models.

The remainder of this paper is structured as follows: In the next section we will provide a concise formulation of the problem to be solved. In Section 3, we will provide background on some of the concepts and methods that we will utilize. This includes background on interval analysis,

fuzzy sets and numbers, fuzzy arithmetic, and Taylor models. Then, in Section 4 we will describe our new approach for the rigorous solution of fuzzy-parameterized, nonlinear dynamic models, with examples and results given in Section 5. Finally in Section 6 we will provide concluding remarks about this work.

2 Problem Statement

We will consider nonlinear dynamic systems described by IVPs of the form

$$\frac{\mathrm{d}\boldsymbol{y}}{\mathrm{d}t} = \boldsymbol{f}(\boldsymbol{y}, \boldsymbol{\theta}), \quad \boldsymbol{y}(t_0) = \boldsymbol{y}_0, \quad t \in [t_0, t_m]. \tag{1}$$

Here the n state variables are represented by the state vector $\boldsymbol{y}$ and have initial values $\boldsymbol{y}_0$. There are p time-invariant parameters represented by the parameter vector $\boldsymbol{\theta}$. The parameters and initial values are uncertain and bounded by the intervals $\boldsymbol{\Theta}$ and $\boldsymbol{Y}_0$, respectively. That is,

$$\boldsymbol{\theta} \in \boldsymbol{\Theta}, \quad \boldsymbol{y}_0 \in \boldsymbol{Y}_0. \tag{2}$$

Additional information about the uncertainties is available in the form of fuzzy numbers or, more generally, in the form of fuzzy sets. That is, for a parameter $\theta_i \in \Theta_i$, the interval Θ_i supports a fuzzy set denoted by $\widetilde{\Theta}_i$, $i = 1, \ldots, p$, and we define the fuzzy parameter vector $\widetilde{\boldsymbol{\Theta}} = (\widetilde{\Theta}_1, \ldots, \widetilde{\Theta}_p)^{\mathrm{T}}$. Similarly, for an initial value $y_{0,i} \in Y_{0,i}$, the interval $Y_{0,i}$ supports a fuzzy set $\widetilde{Y}_{0,i}$, $i = 1, \ldots, n$, and we define the fuzzy initial state vector $\widetilde{\boldsymbol{Y}_0} = (\widetilde{Y}_{0,1}, \ldots, \widetilde{Y}_{0,n})^{\mathrm{T}}$. In these terms, the uncertainties can now be described by

$$\boldsymbol{\theta} \in \widetilde{\boldsymbol{\Theta}}, \quad \boldsymbol{y}_0 \in \widetilde{\boldsymbol{Y}}_0. \tag{3}$$

Fuzzy sets and numbers will be described in more detail in Section 3.2. Our goal is to rigorously propagate these uncertainties, thus computing fuzzy sets $\widetilde{Y}_i(t)$, $i = 1, \ldots, n$, that characterize the uncertainty in the state trajectories $y_i(t)$, $i = 1, \ldots, n$. That is, we seek to determine the fuzzy state vector $\widetilde{\boldsymbol{Y}}(t) = (\widetilde{Y}_1(t), \ldots, \widetilde{Y}_n(t))^{\mathrm{T}}$.

We assume that $\boldsymbol{f}$ is representable by a finite number of standard functions, and that it is sufficiently differentiable for the verified ODE solver used (see Section 4.1). We also note that if the ODE model is nonautonomous, or involves parameters with time dependence of a known form, then such a model can easily be converted into the form of Eq. (1).

3 Background

3.1 Interval Analysis

A real (closed) interval $X = \left[\underline{X}, \overline{X}\right]$ can be defined as the set $X = \left\{x \in \mathbb{R} \mid \underline{X} \leq x \leq \overline{X}\right\}$. Here an underline is used to indicate the lower bound of an interval and an overline is used to indicate the upper bound. The width of an interval is $\mathrm{w}(X) = \overline{X} - \underline{X}$. A real interval vector $\boldsymbol{X} = (X_1, \ldots, X_n)^{\mathrm{T}}$ has n real interval components and can be interpreted geometrically as an n-dimensional rectangle. Basic arithmetic operations with intervals X and Y are defined by $X \circ Y = \{x \circ y \mid x \in X, y \in Y\}, \circ \in \{+, -, \times, \div\}$, with division in the case of $0 \in Y$ allowed only in extensions of interval arithmetic (Hansen & Walster, 2004). Interval versions of the elementary functions are similarly defined. The endpoints of an interval are computed with a directed (outward) rounding; that is, the lower bound is rounded down and the upper bound is rounded up. Thus, interval operations are guaranteed to produce bounds that are rigorous both mathematically and computationally. A number of good introductions to interval analysis and computing with intervals are available (Moore et al., 2009; Hansen & Walster, 2004; Jaulin et al., 2001; Kearfott, 1996; Neumaier, 1990).

For a real function $f(\boldsymbol{x})$ with interval-valued variables $\boldsymbol{x} \in \boldsymbol{X}$, the interval extension $F(\boldsymbol{X})$ can be defined as a real interval that bounds the range of $f(\boldsymbol{x})$ for $\boldsymbol{x} \in \boldsymbol{X}$. One way to compute $F(\boldsymbol{X})$ is to substitute $\boldsymbol{X}$ into the expression for $f(\boldsymbol{x})$ and then to evaluate with interval arithmetic. However, the tightness of these bounds depends on the form of the expression used to evaluate $f(\boldsymbol{x})$. If this is a single-use expression, in which no variable appears more than once, then the exact function range will be obtained (within roundout). However, if any variable appears multiple times, then overestimation of the range may occur. This overestimation is due to the "dependency" problem of interval arithmetic. A variable may take on any value within its interval, but it must take on the *same* value each time it occurs in an expression. Unfortunately, this dependency is not detected when the interval extension is computed using standard interval arithmetic. For example, consider the case $f(x) = (1 - x)/(2 - x)$, with $x \in [0, 1]$. Using interval arithmetic gives $F([0, 1]) = (1 - [0, 1])/(2 - [0, 1]) = [0, 1]/[1, 2] = [0, 1]$. This correctly bounds, but significantly overestimates, the true function range of $[0, 1/2]$. Using a different expression for this function, $f(x) = 1/(x - 2) + 1$, which is now a single-use expression, and evaluating with interval arith-

metic gives $F([0,1]) = 1/([0,1]-2)+1 = 1/[-2,-1]+1 = [-1,-1/2]+1 = [0,1/2]$, the true function range. We could also obtain the true range by noting that, for $x \neq 2$, $f(x)$ is a monotonically decreasing function. Thus, $F([0,1]) = [f(1), f(0)] = [0,1/2]$. For more general cases, there are various other techniques that can be used to sharpen interval function evaluations, including the use of centered forms and interval-splitting techniques. Another source of overestimation that may occur in the use of interval methods is the "wrapping" effect. This occurs when an interval is used to enclose (wrap) a set of results that is not an interval. One approach that can be used to address both the dependency problem and the wrapping effect is the use of Taylor models, which will be described below in Section 3.4.

3.2 Fuzzy Sets and Fuzzy Numbers

Consider an ordinary set $A \subset \mathbb{R}$. One way of expressing the membership of a real number $x \in \mathbb{R}$ in this set is through a "membership function" of the form

$$\mu_A(x) = \begin{cases} 1 & \text{if } x \in A \\ 0 & \text{otherwise.} \end{cases} \tag{4}$$

That is, x is either a member of the set A, and has a membership degree of $\mu_A(x) = 1$, or is not a member of A, and has a membership degree of $\mu_A(x) = 0$. In contrast to this "crisp" set, with $\mu_A(x) \in \{0,1\}$, a "fuzzy" set $\widetilde{A}$ is allowed to also have elements with membership degree between zero and one, i.e., $\mu_{\widetilde{A}}(x) \in [0,1]$. For example (Hanss, 2005), we might define the set T_F of "freezing temperatures" as an ordinary (crisp) set with membership function

$$\mu_{T_F}(x) = \begin{cases} 1 & \text{if } x \leq 0 \\ 0 & \text{if } x > 0 \end{cases} \tag{5}$$

where x indicates temperature in degrees Celsius. But, we might define the set of "cold temperatures" as a fuzzy set $\widetilde{T}_C$ with membership function

$$\mu_{\widetilde{T}_C}(x) = \begin{cases} 1 & \text{if } x \leq -10 \\ 2/3 & \text{if } -10 < x \leq 0 \\ 1/3 & \text{if } 0 < x \leq 10 \\ 0 & \text{if } x > 10. \end{cases} \tag{6}$$

Thus, a temperature of -5 °C belongs to the set of cold temperatures, but with a membership degree of $2/3$. Here, the fuzziness in the set has arisen due to the subjective specification "cold." When someone uses the term "cold" it is possible that they are referring to a temperature below 10 °C. But it is more possible that they are referring to a temperature below 0 °C, and still more possible that they are referring to a temperature below -10 °C.

There are a variety of terms used to describe fuzzy sets and their membership functions. The "support" of a fuzzy set $\widetilde{A}$ in $\mathbb{R}$ is the crisp set of all $x \in \mathbb{R}$ with nonzero membership in $\widetilde{A}$. That is, $\text{support}(\widetilde{A}) = \{x \in \mathbb{R} \mid \mu_{\widetilde{A}}(x) > 0\}$. We will say that x is a member of $\widetilde{A}$ if it is a member of $\text{support}(\widetilde{A})$. That is, $x \in \widetilde{A}$ if $x \in \text{support}(\widetilde{A})$. The "$\alpha$-cut" of $\widetilde{A}$ is the crisp set $(\widetilde{A})_\alpha = \{x \in \mathbb{R} \mid \mu_{\widetilde{A}}(x) \geq \alpha\}$, and the "strong α-cut" is $(\widetilde{A})_{\alpha+} = \{x \in \mathbb{R} \mid \mu_{\widetilde{A}}(x) > \alpha\}$. Thus, $\text{support}(\widetilde{A}) = (\widetilde{A})_{0+}$. Also, this implies that α-cuts are "nested"; that is, $(\widetilde{A})_{\alpha_2} \subseteq (\widetilde{A})_{\alpha_1}$ when $\alpha_1 < \alpha_2$. The α-cut $(\widetilde{A})_1$ is referred to as the "core" of $\widetilde{A}$. In terms of its α-cuts, the membership function of $\widetilde{A}$ can be expressed as

$$\mu_{\widetilde{A}}(x) = \max_{\alpha \in [0,1]} \alpha \mu_{(\widetilde{A})_\alpha}(x). \tag{7}$$

Note that $(\widetilde{A})_\alpha$ is a crisp set, so $\mu_{(\widetilde{A})_\alpha}(x) \in \{0, 1\}$.

A fuzzy set is convex if all of its α-cuts are convex. This implies that all α-cuts, $\alpha \in (0, 1]$ of a convex fuzzy set are closed intervals, as defined in Section 3.1, and means that a convex fuzzy set is unimodal. A fuzzy set is "normal" if the maximum value of its membership function reaches one at one or more points; that is, if its core is nonempty. Following Kaufmann & Gupta (1985), we define a "fuzzy number" as a fuzzy set that is convex and normal, with a core that may be a zero- or nonzero-width interval. Some other authors restrict the term "fuzzy number" to the case that the core is a unique point (zero-width interval), and use the term "fuzzy interval" for the case that the core is a nonzero-width interval. A generic fuzzy number $\widetilde{A}$ is depicted in Fig. 1 by plotting its membership function $\mu_{\widetilde{A}}(x)$. Fig. 1 also identifies the support and core intervals for $\widetilde{A}$, along with an arbitrary α-cut. Some specific types of fuzzy numbers are shown in Fig. 2. These include triangular fuzzy numbers (symmetric and unsymmetric), a trapezoidal fuzzy number, a Gaussian fuzzy number, a "stepped" fuzzy number, and an interval, which is a special case of fuzzy number.

The membership function for a fuzzy uncertainty will depend on the type and amount of information available about the uncertain quantity. If all that is known is an upper bound, a lower

bound, and a "best guess" value, then this knowledge can be represented by a triangular fuzzy number. If the best guess is an interval of values, then this leads to a trapezoidal fuzzy number. In the case of a probabilistic uncertainty, the membership function may be constructed with an appropriate probability density function in mind; for example, a Gaussian fuzzy number (based on a truncated Gaussian probability density function). A stepped (discrete) fuzzy number may arise in various situations, such as the case in which knowledge is obtained by surveys based on experience and/or expertise. For example, say six plant operators are surveyed on the length of time required *in their experience* to complete a certain maintenance task. Two operators estimate a duration of $[15, 17]$ minutes, the third reports $[14, 17]$, the fourth $[15, 18]$, the fifth $[13, 18]$, and the sixth $[14, 19]$. Based on this knowledge, the maintenance time might be represented by the fuzzy number $\widetilde{M}$ whose membership function is shown in Fig. 3. The range $[15, 17]$ is found in all responses and so is assigned the maximum membership degree of one. The ranges $[14, 15]$ and $[17, 18]$ are found in half of the responses and are given a membership degree of $1/2$. The ranges $[13, 14]$ and $[18, 19]$ are found in only one response each, and are given a membership degree of $1/6$. Thus, $\text{core}(\widetilde{M}) = (\widetilde{M})_1 = [15, 17]$, $(\widetilde{M})_{1/2} = [14, 18]$, and $(\widetilde{M})_{1/6} = [13, 19] = \text{support}(\widetilde{M})$. Discrete fuzzy numbers also occur when fuzzy numbers with continuous membership functions are discretized for computational purposes, as discussed in the next section.

3.3 Fuzzy Arithmetic

Operations that can be performed on crisp sets and numbers can be extended to fuzzy sets and numbers using Zadeh's (1975a; 1975b; 1975c) extension principle. For a binary operation $\diamond$ on the fuzzy sets $\widetilde{A}$ and $\widetilde{B}$ with membership functions $\mu_{\widetilde{A}}(x)$ and $\mu_{\widetilde{B}}(y)$, respectively, the extension principle says that the membership function of $\widetilde{C} = \widetilde{A} \diamond \widetilde{B}$ is given by

$$\mu_{\widetilde{C}}(z) = \max_{z = x \diamond y} \min\{\mu_{\widetilde{A}}(x), \mu_{\widetilde{B}}(y)\}, \quad \forall x, y \in \mathbb{R}. \tag{8}$$

This says that to find the membership degree (possibility) of an element z in $\widetilde{C}$, one considers all pairs of x and y for which $x \diamond y = z$. The possibility of each such pair cannot exceed that of its least possible element and so can be expressed as $\min\{\mu_{\widetilde{A}}(x), \mu_{\widetilde{B}}(y)\}$. The possibility of z then corresponds to that of the pair that is most possible. Using such max-min convolutions, arithmetic operations for general fuzzy sets can be implemented (there are also alternative formulations of

the extension principle that can be used, e.g., Dubois & Prade, 1980; Kosheleva et al., 1997). However, this approach is not computationally efficient for the case of fuzzy numbers, as it does not take advantage of their special properties.

While there are various approaches to arithmetic with fuzzy numbers, including the L-R (left-right) representation of Dubois & Prade (1978, 1979), an approach that is now standard (Hanss, 2005) is to exploit the interpretation of a fuzzy number as a nested set of intervals (the α-cuts). Using this approach, it can be shown (Kaufmann & Gupta, 1985) that, for a binary operation with fuzzy numbers $\widetilde{A}$ and $\widetilde{B}$ having membership functions $\mu_{\widetilde{A}}(x)$ and $\mu_{\widetilde{B}}(y)$, respectively, the result $\widetilde{C} = \widetilde{A} \diamond \widetilde{B}$ is a fuzzy number with membership function

$$\mu_{\widetilde{C}}(z) = \max_{\alpha \in [0,1]} \alpha \mu_{(\widetilde{A})_\alpha \diamond (\widetilde{B})_\alpha}(z). \tag{9}$$

This simply says that, for a given value of α, the α-cut of the result $\widetilde{C}$ is given by performing the desired binary operation on the α-cuts of the operands $\widetilde{A}$ and $\widetilde{B}$. That is, $(\widetilde{C})_\alpha = (\widetilde{A})_\alpha \diamond (\widetilde{B})_\alpha$, $\forall \alpha \in (0, 1]$. Thus, since the α-cut of a fuzzy number is a closed interval, arithmetic with fuzzy numbers reduces to arithmetic with intervals, done at each possible α value. This is illustrated in Fig. 4, which shows two stepped fuzzy numbers $\widetilde{A}$ and $\widetilde{B}$ and their sum $\widetilde{C}$. Note, for example, that $(\widetilde{C})_{0.5} = (\widetilde{A})_{0.5} + (\widetilde{B})_{0.5} = [1, 4] + [1, 3] = [2, 7]$ and $(\widetilde{C})_{0.8} = (\widetilde{A})_{0.8} + (\widetilde{B})_{0.8} = [2, 3] + [1, 3] = [3, 6]$. If the membership functions for the operands can be expressed analytically in terms of α, then it may be possible to determine an analytic expression for the resulting fuzzy number. In general, however, fuzzy arithmetic is implemented numerically, with continuous membership functions discretized using several α-cuts. For example, in the software package RAMAS Risk Calc (Ferson, 2002), the fuzzy arithmetic engine is based on discretization using 100 equally spaced α-cuts.

Just as one can define interval extensions of real functions, and evaluate these interval extensions with interval arithmetic to obtain bounds on function values, one can also define fuzzy extensions of real functions and evaluate them using fuzzy arithmetic to obtain bounds on the possibilities of function values. For a real function $f(\boldsymbol{x})$ of n variables $\boldsymbol{x} = (x_1, \ldots, x_n)^{\mathrm{T}}$, with fuzzy-valued variables $x_i \in \widetilde{X}_i$, $i = 1, \ldots, n$, the "fuzzy extension" $\widetilde{F}(\widetilde{X}_1, \ldots, \widetilde{X}_n)$ will have a membership function bounding the possibilities of values of $f(\boldsymbol{x})$. If the inputs $\widetilde{X}_i$, $i = 1, \ldots, n$ are general fuzzy sets, then the fuzzy extension $\widetilde{F}$ can be computed using fuzzy arithmetic based on the max-min convolutions arising from the extension principle, as expressed by Eq. (8). However, if $\widetilde{X}_i$, $i = 1, \ldots, n$ are fuzzy numbers, then $\widetilde{F}$ can be computed using interval extensions at each

α level. That is, $(\widetilde{F})_\alpha = F((\widetilde{X}_1)_\alpha, \ldots, (\widetilde{X}_n)_\alpha)$, $\forall \alpha \in (0,1]$, where F is the interval extension of f, here evaluated over the α-cut intervals $x_i \in (\widetilde{X}_i)_\alpha$, $i = 1, \ldots, n$. If these interval extensions are computed using interval arithmetic, then the dependency problem discussed in Section 3.1 arises, and overestimation of the possibility bounds may occur. To avoid, or at least ameliorate, such overestimation, one can use the same techniques used in the context of interval analysis, such as centered forms, interval splitting, and Taylor models (Section 3.4). However, in the context of fuzzy arithmetic, various other approaches have arisen, such as the "vertex method" (Dong & Shah, 1987) and its various enhancements (e.g., Wood et al., 1992; Otto et al., 1993; Yang et al., 1993; Anile et al., 1995; Chang & Hung, 2006), and the "transformation method" (Hanss, 2002, 2005), itself an extension and generalization of the vertex method. These methods, some of which have been compared by Seng et al. (2007) on numerical test problems, attempt to exploit special properties, such as monotonicity and known extrema, of the function to be bounded over the intervals of interest. By evaluating the function at prescribed points, such as interval vertices and extremal points, it may be possible to bound the function exactly in such cases, as demonstrated previously for a specific function in Section 3.1. In the absence of such special properties, which may be quite difficult to identify *a priori*, function bounding is attempted by sampling the function at an arbitrary set of points, typically based on some grid over the intervals of interest. In general, of course, this will not result in correct function bounds, but in underestimation of the bounds, as noted by Hanss (2005). In the method described here we will use a fundamentally different approach, not based on sampling, that provides mathematically and computationally rigorous possibility bounds in all cases.

3.4 Taylor Models

One approach for addressing the issues of dependency and wrapping that may occur in interval computations, and which may lead to the overestimation of bounds, is the use of Taylor models (Makino & Berz, 1999, 1996, 2003). In this approach, a function is represented using a model consisting of a Taylor polynomial and an interval remainder bound.

The basic idea behind this approach follows directly from the Taylor theorem. Consider a real function $f(\boldsymbol{x})$ that is $(q+1)$ times partially differentiable on the interval $\boldsymbol{X}$ and let $\boldsymbol{x}_0 \in \boldsymbol{X}$. The

Taylor theorem states that for each $\boldsymbol{x} \in \boldsymbol{X}$, there exists a real ζ with $0 < \zeta < 1$ such that

$$f(\boldsymbol{x}) = p_f(\boldsymbol{x} - \boldsymbol{x}_0) + r_f(\boldsymbol{x} - \boldsymbol{x}_0, \zeta), \tag{10}$$

where p_f is a q-th order polynomial (truncated Taylor series) in $(\boldsymbol{x} - \boldsymbol{x}_0)$ and r_f is a remainder, which can be quantitatively bounded over $0 < \zeta < 1$ and $\boldsymbol{x} \in \boldsymbol{X}$ using interval arithmetic or other methods to obtain an interval remainder bound R_f. A q-th order Taylor model $T_f(\boldsymbol{x}) = p_f(\boldsymbol{x} - \boldsymbol{x}_0) + R_f$ for $f(\boldsymbol{x})$ over $\boldsymbol{X}$ then consists of the real-valued polynomial p_f and the interval-valued remainder bound R_f and is denoted by $T_f = (p_f, R_f)$. Note that, by the Taylor theorem, $f(\boldsymbol{x}) \in T_f(\boldsymbol{x})$ for $\boldsymbol{x} \in \boldsymbol{X}$, and thus T_f encloses the range of $f(\boldsymbol{x})$ over $\boldsymbol{X}$.

In practice, it is useful to compute Taylor models of functions by performing Taylor model operations. Arithmetic operations with Taylor models can be done using the operations described by Makino & Berz (1996, 1999, 2003), which include addition, multiplication, reciprocal, and intrinsic functions. Thus, it is possible to start with simple functions such as the constant function $g(\boldsymbol{x}) = k$, for which $T_g = (k, [0, 0])$, and the identity function $g(x_i) = x_i$, for which $T_g = (x_{i0} + (x_i - x_{i0}), [0, 0])$, and to then compute a Taylor model $T_f(\boldsymbol{x})$ for a very complicated function $f(\boldsymbol{x})$. In determining $T_f(\boldsymbol{x})$, the dominant terms are computed using real operations on the coefficients of the Taylor polynomial; thus dependency issues due to interval operations become less significant. The final Taylor model $T_f(\boldsymbol{x})$ must still be bounded for $\boldsymbol{x} \in \boldsymbol{X}$ to bound the range of $f(\boldsymbol{x})$ over $\boldsymbol{X}$, but this can also be done in ways that reduce overestimation (Neumaier, 2003; Lin & Stadtherr, 2007; Makino & Berz, 2004, 2005). It has been reported that, compared to other rigorous range-bounding techniques, the use of Taylor models often provides tighter enclosures for functions with modest to complicated dependencies (Makino & Berz, 1999, 1996; Neumaier, 2003). Since computations with fuzzy numbers can be reduced to computations with intervals, Taylor models can, in general, also be used to reduce overestimation in fuzzy arithmetic. We will use Taylor models here to represent bounds on the solutions of interval-valued IVPs, as described in Section 4.1. Additional applications, as well as limitations, of Taylor models are discussed in more detail elsewhere (Neumaier, 2003).

4 Solution Method

In this section, we describe a new approach for solving the problem posed in Section 2, namely

the propagation of fuzzy uncertainties in solving IVPs for nonlinear ODE systems. A key requirement in developing this approach is that, unlike other methods for addressing this problem, the computed possibility bounds be rigorous. Since, as discussed above, computation with fuzzy numbers can be reduced to computations with intervals, we begin by discussing the propagation of interval uncertainties in nonlinear dynamic systems, and by outlining the specific approach that will be used here for the interval computations.

4.1 Interval Uncertainties

Consider the problem stated in Eqs. (1) and (2). This is an IVP for a nonlinear ODE with interval-valued parameters and initial states. Using interval methods (also called validated methods or verified methods) for ODEs, it is possible to determine mathematically and computationally guaranteed bounds on the state trajectories. Traditional interval methods use two processes (phases) at each integration step. In the first process, existence and uniqueness of the solution are proven, and a rough enclosure of the solution, valid over the entire integration time step, is computed. In the second process, a tighter enclosure of the solution, valid at the endpoint of the time step, is computed. In general, both processes are implemented by applying interval Taylor series (ITS) expansions with respect to time, using automatic differentiation to obtain the Taylor coefficients. A thorough review of the traditional interval methods has been given by Nedialkov (1999), and more recent work has been reviewed by Neher et al. (2007). For addressing this problem, there are several packages available, involving a variety of methods; these include VNODE (Nedialkov, 1999; Nedialkov et al., 2001), COSY VI (Berz & Makino, 1998), and ValEncIA-IVP (Rauh et al., 2009). In this study, we will use the recently developed solver VSPODE (Lin & Stadtherr, 2007). The method makes use, in a novel way, of the Taylor model approach (Makino & Berz, 1996, 1999, 2003) to deal with the dependency and wrapping issues involving the uncertain quantities (parameters and initial states).

Assuming an interval enclosure $\boldsymbol{Y}_j$ of the state variables $\boldsymbol{y}_j = \boldsymbol{y}(t_j)$, an integration step in VSPODE determines a time step $h_j = t_{j+1} - t_j$ and an interval enclosure $\boldsymbol{Y}_{j+1}$ of the state variables at t_{j+1}. In the first phase of the method, a coarse enclosure $\widehat{\boldsymbol{Y}}_j$ is determined such that a unique solution $\boldsymbol{y}(t) \in \widehat{\boldsymbol{Y}}_j$ is guaranteed to exist over the time interval $[t_j, t_{j+1}]$ for every $\boldsymbol{y}_j \in \boldsymbol{Y}_j$ and every $\boldsymbol{\theta} \in \boldsymbol{\Theta}$. This is done with a high-order ITS with respect to time, using the Picard-Lindelöf

operator and Banach fixed-point theorem. The time step used can be specified, but may be reduced if necessary, or an automatic step size procedure can be used. This represents an extension, to parametric ODEs, of the traditional interval approach used in VNODE.

In the second phase of the method, Taylor models in terms of the uncertain quantities are used. First, the uncertain quantities (initial values and parameters) are expressed as Taylor model identity functions $\boldsymbol{T}_{\boldsymbol{y}_0}$ and $\boldsymbol{T}_{\boldsymbol{\theta}}$. Then, Taylor models $\boldsymbol{T}_{\boldsymbol{f}^{[i]}}$ of the ITS coefficients $\boldsymbol{f}^{[i]}(\boldsymbol{y}_j, \boldsymbol{\theta})$ are obtained by using Taylor model operations to compute $\boldsymbol{T}_{\boldsymbol{f}^{[i]}} = \boldsymbol{f}^{[i]}(\boldsymbol{T}_{\boldsymbol{y}_j}, \boldsymbol{T}_{\boldsymbol{\theta}})$. Now using the ITS expansion for $\boldsymbol{y}_{j+1}$, with coefficients given by $\boldsymbol{T}_{\boldsymbol{f}^{[i]}}$, and incorporating an approach for using the mean value theorem on Taylor models, one can obtain $\boldsymbol{T}_{\boldsymbol{y}_{j+1}}(\boldsymbol{y}_0, \boldsymbol{\theta})$, a Taylor model of $\boldsymbol{y}_{j+1}$ in terms of the parameters $\boldsymbol{\theta}$ and initial states $\boldsymbol{y}_0$. In this process, the wrapping effect of traditional interval methods is reduced by using a new type of Taylor model that uses a parallelepiped (as opposed to interval) remainder bound (Lin & Stadtherr, 2007). The Taylor model $\boldsymbol{T}_{\boldsymbol{y}_{j+1}}(\boldsymbol{y}_0, \boldsymbol{\theta})$ is an explicit analytical expression for $\boldsymbol{y}_{j+1} = \boldsymbol{y}(t_{j+1})$ in terms of the initial states $\boldsymbol{y}_0$ and parameters $\boldsymbol{\theta}$, which is valid for all $\boldsymbol{y}_0 \in \boldsymbol{Y}_0$ and all $\boldsymbol{\theta} \in \boldsymbol{\Theta}$. The interval state bounds $\boldsymbol{Y}_{j+1}$ can now be obtaining by bounding $\boldsymbol{T}_{\boldsymbol{y}_{j+1}}(\boldsymbol{y}_0, \boldsymbol{\theta})$ over $\boldsymbol{y}_0 \in \boldsymbol{Y}_0$ and $\boldsymbol{\theta} \in \boldsymbol{\Theta}$. These bounds are mathematically and computationally guaranteed. Complete details of the method outlined briefly here are given by Lin & Stadtherr (2007). Other interesting ideas for using Taylor models in state bounding have been described recently by Sahlodin & Chachuat (2011a,b).

4.2 Fuzzy Uncertainties

Consider the problem stated in Eqs. (1) and (3). Now the uncertainties in the ODE parameters and initial states are represented by the fuzzy set vectors $\widetilde{\boldsymbol{\Theta}}$ and $\widetilde{\boldsymbol{Y}}_0$ rather than the intervals $\boldsymbol{\Theta}$ and $\boldsymbol{Y}_0$. We will consider methods for three cases of this problem: 1. The uncertainties are general fuzzy sets; 2. The uncertainties are discrete fuzzy numbers represented by a relatively small number of α-cuts; 3. The uncertainties are discrete fuzzy numbers represented by a relatively large number of α-cuts. The third case includes the case of membership functions that are continuous functions of α, since in practice these are discretized using a large number of α-cuts.

4.2.1 Method 1: General fuzzy sets

For this most general case, we apply VSPODE with the interval parameter input $\boldsymbol{\Theta} =$

$\text{support}(\widetilde{\boldsymbol{\Theta}}) = (\text{support}(\widetilde{\Theta}_1), \ldots, \text{support}(\widetilde{\Theta}_p))^{\mathrm{T}}$ and the interval initial state input $\boldsymbol{Y}_0 = \text{support}(\widetilde{\boldsymbol{Y}}_0)$. At the j-th integration time step (beginning with $j = 1$ and finishing with $j = m$), a Taylor model $\boldsymbol{T}_{\boldsymbol{y}_j}(\boldsymbol{y}_0, \boldsymbol{\theta})$ for $\boldsymbol{y}_j = \boldsymbol{y}(t_j)$ valid for all $\boldsymbol{y}_0 \in \widetilde{\boldsymbol{Y}}_0$ and all $\boldsymbol{\theta} \in \widetilde{\boldsymbol{\Theta}}$ is obtained (since all elements of a fuzzy set are elements of its support interval). Since $\boldsymbol{T}_{\boldsymbol{y}_j}(\boldsymbol{y}_0, \boldsymbol{\theta})$ is an explicit polynomial function plus an interval remainder bound, a fuzzy set vector $\widetilde{\boldsymbol{Y}}_j$ characterizing the uncertainty in $\boldsymbol{y}_j$ can now be computed from $\widetilde{\boldsymbol{Y}}_j = \boldsymbol{T}_{\boldsymbol{y}_j}(\widetilde{\boldsymbol{Y}}_0, \widetilde{\boldsymbol{\Theta}})$ using fuzzy arithmetic. That is, the fuzzy parameter $\widetilde{\boldsymbol{\Theta}}$ and fuzzy initial state $\widetilde{\boldsymbol{Y}}_0$ are substituted into the Taylor model for the states and fuzzy arithmetic based on the max-min convolutions arising from the extension principle, as expressed by Eq. (8), is used to compute the fuzzy state $\widetilde{\boldsymbol{Y}}_j$. At completion of all m time steps, this yields the complete fuzzy trajectory $\widetilde{\boldsymbol{Y}}(t_j) = \widetilde{\boldsymbol{Y}}_j$, $j = 1, \ldots, m$.

This approach is completely general. However, in most cases of interest, the fuzzy sets used to represent uncertainties are convex and normal, that is, they are fuzzy numbers. The method described above does not take advantage of the special properties of fuzzy numbers. We will concentrate here on methods for uncertainties that are expressed as fuzzy numbers.

4.2.2 Method 2: Fuzzy numbers with small number of α-cuts

For this case, we assume that the components of $\widetilde{\boldsymbol{\Theta}}$ and $\widetilde{\boldsymbol{Y}}_0$ are fuzzy numbers that can be represented using a relatively small number of α-cuts. Say there are a total of r α-cuts needed to represent both $\widetilde{\boldsymbol{\Theta}}$ and $\widetilde{\boldsymbol{Y}}_0$. These α-cuts are at α_1, $\alpha_2, \ldots, \alpha_{r-1}$ and α_r, with $0 < \alpha_1 < \alpha_2 < \ldots < \alpha_{r-1} < \alpha_r = 1$. For example, representation of the fuzzy number $\widetilde{A}$ depicted in Fig. 4 requires $r = 5$ with $\alpha_1 = 0.3$, $\alpha_2 = 0.4$, $\alpha_3 = 0.6$, $\alpha_4 = 0.7$ and $\alpha_5 = 1$. Note that the α-cut at α_1 corresponds to the support of the fuzzy number, and the α-cut at α_r to the core.

As explained in Section 3.3, arithmetic with fuzzy numbers reduces to arithmetic with intervals, done at each α value used to represent the fuzzy numbers. Thus, we can compute the fuzzy trajectory $\widetilde{\boldsymbol{Y}}_j$, $j = 1, \ldots, m$ one α-cut at a time using VSPODE. Consider the k-th α-cut (at α_k). The corresponding α-cut of $\widetilde{\boldsymbol{\Theta}}$ is $(\widetilde{\boldsymbol{\Theta}})_{\alpha_k} = ((\widetilde{\Theta}_1)_{\alpha_k}, \ldots, (\widetilde{\Theta}_p)_{\alpha_k})^{\mathrm{T}}$, and the corresponding α-cut of $\widetilde{\boldsymbol{Y}}_0$ is $(\widetilde{\boldsymbol{Y}}_0)_{\alpha_k} = ((\widetilde{Y}_{0,1})_{\alpha_k}, \ldots, (\widetilde{Y}_{0,n})_{\alpha_k})^{\mathrm{T}}$. Now apply VSPODE with interval inputs $\boldsymbol{\Theta} = (\widetilde{\boldsymbol{\Theta}})_{\alpha_k}$ and $\boldsymbol{Y}_0 = (\widetilde{\boldsymbol{Y}}_0)_{\alpha_k}$. This will result in rigorous bounds on $(\widetilde{\boldsymbol{Y}}_j)_{\alpha_k}$ at each time step $j = 1, \ldots, m$. To obtain the complete fuzzy trajectory, then requires r calls to VSPODE, one for each α-cut. Examples of this approach are given below in Sections 5.1 and 5.2. As long as the number of α-cuts is relatively

small, this will be an efficient approach providing fuzzy trajectories that reflect relatively tight possibility bounds. However, if the number of α-cuts is relatively large, requiring a large number of calls to VSPODE, this approach can become very costly computationally. Thus, we consider next an approach that limits the number of calls to VSPODE when there is a large number of α-cuts.

4.2.3 Method 3: Fuzzy numbers with large number of α-cuts

Again we assume that the components of $\widetilde{\boldsymbol{\Theta}}$ and $\widetilde{\boldsymbol{Y}}_0$ are fuzzy numbers that can be represented using r α-cuts, as described above. However, now we also assume that r is a relatively large number. This is the situation encountered when fuzzy numbers with continuous membership functions are discretized for purposes of performing fuzzy arithmetic. Instead of using the Method 2 approach, we want an approach that will limit the number of calls to VSPODE. To do this we will make use of the nesting property of α-cuts, which says that $(\widetilde{A})_{\alpha_k} \subseteq (\widetilde{A})_{\alpha_i}$ when $\alpha_i < \alpha_k$. Say we use VSPODE on the α-cut at α_i. This will result in the computation of the rigorous state bounds $(\widetilde{\boldsymbol{Y}}_j)_{\alpha_i}$ at each time step $j = 1, \ldots, m$. To obtain each such $(\widetilde{\boldsymbol{Y}}_j)_{\alpha_i}$, VSPODE first determines a Taylor model $\boldsymbol{T}_{\boldsymbol{y}_j}(\boldsymbol{y}_0, \boldsymbol{\theta})$ valid for all $\boldsymbol{y}_0 \in (\widetilde{\boldsymbol{Y}}_0)_{\alpha_i}$ and all $\boldsymbol{\theta} \in (\widetilde{\boldsymbol{\Theta}})_{\alpha_i}$ (see Section 4.1). We will denote this Taylor model as $\boldsymbol{T}^{\alpha_i}_{\boldsymbol{y}_j}(\boldsymbol{y}_0, \boldsymbol{\theta})$. The state bound $(\widetilde{\boldsymbol{Y}}_j)_{\alpha_i}$ is then computed using $(\widetilde{\boldsymbol{Y}}_j)_{\alpha_i} = \boldsymbol{T}^{\alpha_i}_{\boldsymbol{y}_j}((\widetilde{\boldsymbol{Y}}_0)_{\alpha_i}, (\widetilde{\boldsymbol{\Theta}})_{\alpha_i})$. Now say we want to determine $(\widetilde{\boldsymbol{Y}}_j)_{\alpha_k}$ at each time step $j = 1, \ldots, m$, with $\alpha_k > \alpha_i$. Since $(\widetilde{\boldsymbol{Y}}_0)_{\alpha_k} \subseteq (\widetilde{\boldsymbol{Y}}_0)_{\alpha_i}$ and $(\widetilde{\boldsymbol{\Theta}})_{\alpha_k} \subseteq (\widetilde{\boldsymbol{\Theta}})_{\alpha_i}$ the Taylor model computed previously for α_i is still valid. Thus, for α_k it is not necessary to use VSPODE to determine a new Taylor model, and we can get each $(\widetilde{\boldsymbol{Y}}_j)_{\alpha_k}$ simply from the Taylor model evaluation $(\widetilde{\boldsymbol{Y}}_j)_{\alpha_k} = \boldsymbol{T}^{\alpha_i}_{\boldsymbol{y}_j}((\widetilde{\boldsymbol{Y}}_0)_{\alpha_k}, (\widetilde{\boldsymbol{\Theta}})_{\alpha_k})$. In re-using the Taylor model from α_i there is, however, a tradeoff. The resulting state bounds for the α_k-cut will be rigorous, but not quite as tight as if they were calculated from a new run of VSPODE and thus from a new Taylor model $\boldsymbol{T}^{\alpha_k}_{\boldsymbol{y}_j}$.

In the examples shown below, we will consider some possible strategies for dealing with this tradeoff. On one extreme is the case in which VSPODE is used only once, on the α_1-cut, corresponding to the support of the fuzzy number input. The Taylor model $\boldsymbol{T}^{\alpha_1}_{\boldsymbol{y}_j}(\boldsymbol{y}_0, \boldsymbol{\theta})$ can then be re-used at all other α-cuts. This will involves the least computational work, but also the greatest overestimation of the state possibility bounds. The other extreme corresponds to Method 2, as discussed above, which will involve the most computational work, but the least overestimation of bounds. We will use the numerical examples in Sections 5.3 and 5.4 to look at these two extremes

and at ways to compromise between them. A systematic procedure for implementing Method 3 will be outlined in Section 5.4.

5 Computational Studies

In this section, we apply the methods outlined above to a number of examples. Each example involves a nonlinear ODE model that has parameters and/or initial conditions that are uncertain and represented by fuzzy numbers. The first two examples involve ecological dynamics and fuzzy numbers with small number of α-cuts. The remaining examples involve bioreactor dynamics and fuzzy numbers with continuous membership functions. Since our solution methods are designed to be general-purpose, we will not attempt to exploit any special properties in the example problems.

The solution methods were implemented using a C++ wrapper around the VSPODE library, which was set to use the default ITS truncation order ($k = 17$) and Taylor model order ($q = 5$). All the example problems were solved on a dual-core AMD Opteron™ Model 1214 processor (2.2 GHz) running Ubuntu 11.04.

5.1 Example 1: Two-Species Competition Model

For this example, we consider a two-species model of competition dynamics over a period of $t \in [0, 100]$ days. The model of interest is given by

$$\frac{\mathrm{d}y_1}{\mathrm{d}t} = r_1 y_1 \left(1 - \frac{y_1 + a_{12} y_2}{K_1}\right) \tag{11}$$

$$\frac{\mathrm{d}y_2}{\mathrm{d}t} = r_2 y_2 \left(1 - \frac{y_2 + a_{21} y_1}{K_2}\right), \tag{12}$$

where y_1 and y_2 represent the populations of the two competing species. Here r_1 and r_2 are the intrinsic species growth rates per capita, and K_1 and K_2 are the carrying capacities for each species in the absence of competition. The competition parameters a_{12} and a_{21} represent the impact of species 2 on species 1 and the impact of species 1 on species 2, respectively. This model represents a modification of the logistic population model to account for competition and is commonly referred to as the Lotka-Volterra competition model. The initial states are $y_{0,1} = 150$ and $y_{0,2} = 130$. Some parameters have known crisp values: $K_1 = 560$, $K_2 = 202$, $r_1 = 1$ day^{-1}

and $a_{12} = 2.66$. The parameters r_2 and a_{21} are uncertain and represented by fuzzy numbers. For $r_2 = \theta_1$, the fuzzy number input is given by support$(\widetilde{\Theta}_1) = (\widetilde{\Theta}_1)_{1/3} = [0.56, 0.64]$ day^{-1}, $(\widetilde{\Theta}_1)_{2/3} = [0.575, 0.625]$ day^{-1}, and $(\widetilde{\Theta}_1)_1 = [0.59, 0.61]$ day^{-1}. For $a_{21} = \theta_2$, the fuzzy number input is given by support$(\widetilde{\Theta}_2) = (\widetilde{\Theta}_2)_{1/3} = [0.305, 0.315]$, $(\widetilde{\Theta}_2)_{2/3} = [0.307, 0.313]$, and $(\widetilde{\Theta}_2)_1 = [0.309, 0.311]$. The membership functions for these fuzzy number inputs are depicted in Fig. 5. Since the fuzzy inputs are represented by only three α-cuts, we applied Method 2, as described in Section 4.2.2, with $r = 3$, $\alpha_1 = 1/3$, $\alpha_2 = 2/3$, and $\alpha_3 = 1$.

Selected results are shown in Fig. 6, which shows the fuzzy trajectories at 4, 20, 40, 60 and 80 days. The fuzzy trajectories are indicated schematically by showing flipped and rotated plots of the membership functions for the state variables. The correspondence between this schematic representation and the membership function plot is shown in detail for the case of $t = 40$ days. The dotted curves in Fig. 6 show the bounds on the states computed by VSPODE for the case of a purely interval uncertainty, based on the support intervals for the fuzzy number inputs. Even though the fuzzy number inputs were symmetric, the fuzzy state outputs can be seen to be slightly asymmetric, showing a bias towards higher population of species 2 (and lower population of species 1) as being more possible. The computation time required to compute the state membership functions at $t = 80$ was 3.5 s (less at smaller values of t).

5.2 Example 2: Predator-Prey Model

For this example, we use a two-species model of predator-prey dynamics over a period of $t \in [0, 25]$ days. This system is described by the ODE system

$$\frac{\mathrm{d}y_1}{\mathrm{d}t} = \theta_1 y_1 (1 - y_2) \tag{13}$$

$$\frac{\mathrm{d}y_2}{\mathrm{d}t} = \theta_2 y_2 (y_1 - 1), \tag{14}$$

where y_1 represents the prey population and y_2 the predator population. The parameters θ_1 and θ_2 may be regarded as interaction coefficients. This is a version of the Lotka-Volterra predator-prey model, and is widely used as a numerical test problem in nonlinear dynamics. The state trajectories can be quite sensitive to small changes in the parameter values. Here the parameters are uncertain and represented by fuzzy numbers. For θ_1, the fuzzy number input is given by support$(\widetilde{\Theta}_1) = (\widetilde{\Theta}_1)_{1/3} = [2.99, 3.01]$ day^{-1}, $(\widetilde{\Theta}_1)_{2/3} = [2.995, 3.005]$ day^{-1}, and $(\widetilde{\Theta}_1)_1 =$

$[2.999, 3.001]$ day^{-1}. For θ_2, the fuzzy number input is given by support$(\widetilde{\Theta}_2) = (\widetilde{\Theta}_2)_{1/3} = [0.99, 1.01]$ day^{-1}, $(\widetilde{\Theta}_2)_{2/3} = [0.995, 1.005]$ day^{-1}, and $(\widetilde{\Theta}_2)_1 = [0.999, 1.001]$ day^{-1}. The initial states are $y_{0,1} = 1.2$ and $y_{0,2} = 1.1$.

Since again the fuzzy inputs are represented by only three α-cuts, we again applied Method 2. Selected results are shown in Fig. 7, which shows the fuzzy trajectories at 20.5, 21.2, 22.2, 23.5 and 24.2 days. The membership function plot is shown in detail for the case of $t = 22.2$ days. The dotted curves in Fig. 7 indicate the state bounds computed by VSPODE for the case of a purely interval uncertainty, corresponding to the support intervals for the fuzzy number inputs. Even though the fuzzy number inputs were again symmetric, in this case the fuzzy state outputs can be seen to be highly asymmetric, with the nature of this asymmetry varying with time. For example, looking at the membership functions for the predator population (y_2) near its extrema, the interval of most possible populations shifts towards relatively larger values near the maximum and towards relatively smaller values near the minimum. The computation time required to compute the state membership functions at $t = 24.2$ days was 0.5 s (less at smaller values of t).

By using VSPODE to integrate the sensitivity equations for this problem, together with the original ODEs, over the uncertainty intervals of interest, it can be shown that the states do not vary monotonically with respect to all of the parameters over the entire time span. As discussed above, this means that an approach based on sampling of the fuzzy inputs will not rigorously bound the fuzzy trajectories (Hanss, 2005). At best, a sampling approach will yield an inner estimate of the state bounds for a given α-cut, with the tightness of the bounds determined, in general, by the effort expended in sampling. On the other hand, for a problem in which the states do vary monotonically with respect to the parameters (Example 1 can be shown to be such a problem), it is possible to obtain rigorous and tight bounds by sampling, provided the samples include the endpoints of the input α-cut intervals. However, the user will not know that the results are rigorous unless the monotonicity property has been verified *a priori*. In general, this requires the integration of the sensitivity equations, together with the original ODE, using an approach that rigorously bounds the sensitivities over the specified uncertainty intervals (this can be done using VSPODE). Using the approach described here, which does not involve sampling, we can directly and confidently obtain rigorous bounds on the fuzzy trajectories for any problem, whether or not the states vary monotonically with the parameters. In general, these bounds may overestimate the

exact bounds. However, if there is *a priori* knowledge of monotonic sensitivity behavior, this can be exploited to obtain the best possible bounds.

5.3 Example 3: Two-State Bioreactor Models

The dynamics of a continuous, well-mixed bioreactor (chemostat) in which biomass of a single organism is produced and there is a single limiting nutrient (substrate) can be described by the ODE system

$$\frac{\mathrm{d}X}{\mathrm{d}t} = (\mu - aD)X, \tag{15}$$

$$\frac{\mathrm{d}S}{\mathrm{d}t} = D(S_\mathrm{f} - S) - k\mu X, \tag{16}$$

where X and S are the (real-valued) concentrations of biomass and substrate, respectively. Here μ is the specific growth rate of biomass, a function of S that will be given below, D is the dilution rate (space velocity), a is the biomass washout fraction, k is the inverse yield coefficient, and S_f is the substrate feed concentration. We will consider a time horizon of 20 h.

5.3.1 Monod kinetics

We first consider the case of Monod kinetics, with the specific growth rate given by

$$\mu = \frac{\mu_{\max} S}{K_\mathrm{S} + S}. \tag{17}$$

Here $\mu_{\max}$ is the maximum specific growth rate and K_S is the half-saturation constant. Fixed parameter values for this problem are $a = 0.5$, $k = 10.53$, $S_\mathrm{f} = 5.7$ g/L, and $\mu_{\max} = 1.2\ \mathrm{h}^{-1}$. The initial states are also fixed, at $X_0 = 0.829$ g/L and $S_0 = 0.8$ g/L. The parameters D and K_S will be treated as uncertain and represented by symmetric trapezoidal fuzzy numbers, as indicated in Fig. 8. A trapezoidal fuzzy number can be specified by giving its support and core intervals. For D, $\mathrm{support}(\widetilde{D}) = [0.35, 0.37]\ \mathrm{h}^{-1}$ and $\mathrm{core}(\widetilde{D}) = (\widetilde{D})_1 = [0.35667, 0.36333]\ \mathrm{h}^{-1}$. For K_S, $\mathrm{support}(\widetilde{K}_\mathrm{S}) = [6.8, 7.2]$ g/L and $\mathrm{core}(\widetilde{K}_\mathrm{S}) = (\widetilde{K}_\mathrm{S})_1 = [6.93333, 7.06667]$ g/L. Since the fuzzy inputs have continuous membership functions, they must be discretized for purposes of numerical fuzzy arithmetic. We will treat these continuous membership functions by discretizing them into 100 equally-spaced α-cuts (Ferson, 2002); thus, $r = 100$ with $\alpha_1 = 0.01$, $\alpha_1 = 0.02$, …, $\alpha_{100} = 1.0$.

Since there are a large number of α-cuts, we applied Method 3, as described in Section 4.2.3, and used VSPODE only once, on the support intervals for the fuzzy inputs. Thus, results for all α-cuts were based on a single Taylor model, computed at $\alpha_1 = 0.01$. Selected results are shown in Fig. 9, which shows the fuzzy trajectories at 1.8, 4.5, 8.0, 12.5 and 17.4 h. The membership function plot is shown in detail for the case of $t = 8.0$ h. The dotted curves in Fig. 9 are the state bounds computed by VSPODE based on the support intervals for the fuzzy inputs.

For comparison, we also applied Method 2, running VSPODE $r = 100$ times, thus using 100 different Taylor models, one for each α-cut. This will provide tighter possibility bounds than Method 3, but at higher computational cost. To quantify the relative difference in bound tightness between the two methods, and provide a measure of performance for Method 3 in this regard, we use two quantities: 1) Area Ratio and 2) Maximum Interval Ratio. Both measures are based on the membership function curve for a particular state variable at a particular time. The Area Ratio is based on the area under the membership function curve, and is simply the ratio of this area based on Method 3 to this area based on Method 2. In principle the Area Ratio will always be greater than one, with values closer to one indicating better performance. The Maximum Interval Ratio is based on the ratio of the width of the state possibility interval for a particular α-level as determined by Method 3 to the width of this interval as determined by Method 2 for the same α-level. The maximum value of this ratio is the Maximum Interval Ratio. Again, this value will always be greater than one, with values closer to one indicating better performance. The Area Ratio provides a global measure of overestimation, while the Maximum Interval Ratio provides a local measure. The tradeoffs between the Methods 2 and 3 for this problem can be seen in Table 1, which shows the computation time for each method and the Area Ratio and Maximum Interval Ratio based on X and S at $t = 20$ h. It is clear that, for this problem, Method 3 performs very well. It is two orders of magnitude faster than Method 2, and provides possibility bounds nearly as tight as Method 2.

5.3.2 Haldane kinetics

As a second example involving a two-state bioreactor, we will use Haldane kinetics, with the

specific growth rate given by

$$\mu = \frac{\mu_{\max} S}{K_S + S + K_I S^2}. \tag{18}$$

Here there is an additional kinetic parameter, the inhibition constant K_I. Fixed parameter values for this problem are $a = 0.5$, $k = 10.53$, $S_f = 5.7$ g/L, $D = 0.3$ h^{-1}, $\mu_{\max} = 1.2$ h^{-1}, and $K_S = 7.0$ g/L. The initial substrate concentrate is fixed at $S_0 = 0.8$ g/L, but the initial concentration of biomass is uncertain. It is given by the trapezoidal fuzzy number specified by support$(\widetilde{X}_0) = [0.825, 0.835]$ g/L and core$(\widetilde{X}_0) = [0.82833, 0.83167]$ g/L. The inhibition constant is also uncertain, and it is given by the trapezoidal fuzzy number specified by support$(\widetilde{K}_I) = [1.48, 1.52]$ L/g and core$(\widetilde{K}_I) = [1.49333, 1.50667]$ L/g.

Again, we applied Method 3. Selected results are shown in Fig. 10, which shows the fuzzy trajectories at 1.5, 2.9, 6.5, 11.2 and 16.0 h, and state bounds (dotted curves) computed by VSPODE using the support intervals for the fuzzy inputs. The membership function plot is shown in detail for the case of $t = 11.2$ h. The tradeoffs between the Methods 2 and 3 for this problem are given in Table 1. It is clear that, for this problem also, Method 3 performs very well relative to Method 2.

5.4 Example 4: Three-State Bioreactor Model

In this bioreactor model (Henson & Seborg, 1997), the consumption of substrate (concentration S) by cells (concentration X) results in the formation of a product (concentration P) that inhibits the growth of the cells. The ODE system is

$$\frac{dX}{dt} = (\mu - D)X \tag{19}$$

$$\frac{dS}{dt} = D(S_f - S) - \frac{\mu X}{Y} \tag{20}$$

$$\frac{dP}{dt} = -DP + (\gamma\mu + \beta)X, \tag{21}$$

where the specific biomass growth rate is given by

$$\mu = \frac{\mu_{\max}(1 - P/P_m)S}{(K_S + S)} \tag{22}$$

Here Y is the biomass yield coefficient, P_m is a normalization factor, γ and β are product yield parameters, and the other parameters are as defined in the previous section. We will consider a time horizon of 20 h.

Fixed parameter values for this example are $\gamma = 0.2$, $\beta = 3.0$ h^{-1}, $S_f = 20$ g/L, $P_m = 50$ g/L, $Y = 0.42$, and $K_S = 5.065$ g/L. Fixed initial states are $S_0 = 5.0$ g/L and $P_0 = 15.0$ g/L. The remaining parameters and initial state are uncertain and given by symmetric trapezoidal fuzzy numbers. For D, support$(\widetilde{D}) = [0.20, 0.22]$ h^{-1} and core$(\widetilde{D}) = [0.20667, 0.21333]$ h^{-1}. For μ_{max}, support$(\widetilde{\mu}_{max}) = [4.64, 4.66]$ h^{-1} and core$(\widetilde{\mu}_{max}) = [4.64667, 4.65333]$ h^{-1}. For X_0, support$(\widetilde{X}_0) = [6.40, 6.60]$ g/L and core$(\widetilde{X}_0) = [6.46667, 6.53333]$ g/L. Again we will discretize these continuous membership functions into 100 equally-spaced α-cuts, so $r = 100$ with $\alpha_1 = 0.01$, $\alpha_1 = 0.02$, ..., $\alpha_{100} = 1.0$.

As in the previous example, we computed the fuzzy states using Method 2 with $r = 100$ Taylor models, one for each α-level, and using Method 3 with only one Taylor model, at $\alpha_1 = 0.01$, and compared the results in terms of computational performance. The results of this comparison are shown in the first two rows of Table 2. While, Method 3 is much faster, as expected, it also leads to a nontrivial overestimation of the possibility bounds relative to Method 2, as indicated by the Area Ratio of 1.0724 and Maximum Interval Ratio of 1.1976 (both ratios represent the average over all three state variables at $t = 16$ h).

To reduce the overestimation by Method 3 we can simply increase the number of Taylor models used from one to some larger number. We will first concentrate on what happens when the number of Taylor models used in Method 3 is increased to two. The performance in terms of overestimation will depend on which α-level is chosen for the second application of VSPODE and the second Taylor model. We will refer to this α-level as the "reset level", and will denote this value as α^*. The effect of the reset level can be seen clearly in Table 2, which shows that the least overestimation was observed when the second Taylor model was obtained at α-levels in the range of 0.2 to 0.4. This result is not surprising since, in evaluating interval function extensions using interval arithmetic, overestimation will be greater when the diameters of the interval inputs are greater. Thus, there is more to gain by obtaining the more accurate Taylor model at a relatively small α value, at which the diameter of the input α-cut intervals is still relatively large. The exact α value that leads to best performance with a second Taylor model will clearly vary from problem to problem. Based on our experience with this and other problems, however, the use of $\alpha = 0.2$ for evaluation of the second Taylor model is a good heuristic choice, as it tends to result in the smallest Area Ratio, a global measure of overestimation.

We can now consider using three or more Taylor models to further reduce overestimation by Method 3. For this purpose, we suggest recursive use of the heuristic suggested above. That is, if $\alpha^{(2)} = \alpha^* = 0.2$ denotes the α-level for the second Taylor model, then $\alpha^{(3)} = \alpha^{(2)} + \alpha^*(1 - \alpha^{(2)}) = 0.36$ is the location for the third Taylor model, $\alpha^{(4)} = \alpha^{(3)} + \alpha^*(1 - \alpha^{(3)}) = 0.488$ is (rounded to the nearest discrete α-level of 0.49) the location for the fourth, etc. In general then, the α-level $\alpha^{(u+1)}$ for the $(u+1)$-th Taylor model will be given by $\alpha^{(u+1)} = \alpha^{(u)} + \alpha^*(1 - \alpha^{(u)})$ for $u \geq 2$.

We can now suggest a systematic procedure for applying Method 3. Convergence of this procedure will be monitored by considering the relative change, when an additional Taylor model evaluation is done, in the area under the membership function curves for the state variables (at a specified time). We will denote by $A^{(u)}$ the area under the state membership functions at the specified time, averaged over all states, when u Taylor models have been used to obtain the membership functions. If the "relative area difference" $R_{\mathrm{A}}^{(u)} = (A^{(u-1)} - A^{(u)})/A^{(u-1)} < \epsilon$, where ϵ is a specified tolerance, then we will stop the procedure and use the result obtained using u Taylor models.

An outline of the algorithm is as follows:

1. Initialize
   (a) Assign a value for the reset level α^*.
   (b) Assign a value for the stopping tolerance ϵ.
   (c) Run VSPODE and obtain a first Taylor model $\boldsymbol{T}_{\boldsymbol{y}_j}^{\alpha^{(1)}}$ at $\alpha^{(1)} = \alpha_1$. This is the α-level corresponding to the support of the fuzzy number inputs. For all $k \in [1, r]$, compute $(\widetilde{\boldsymbol{Y}}_j)_{\alpha_k}$ at each time step $j = 1, \ldots, m$ using $(\widetilde{\boldsymbol{Y}}_j)_{\alpha_k} = \boldsymbol{T}_{\boldsymbol{y}_j}^{\alpha^{(1)}}((\widetilde{\boldsymbol{Y}}_0)_{\alpha_k}, (\widetilde{\boldsymbol{\Theta}})_{\alpha_k})$. Determine $A^{(1)}$.
   (d) Set $u = 2$ and $\alpha^{(2)} = \alpha^*$.
2. Run VSPODE and obtain a Taylor model $\boldsymbol{T}_{\boldsymbol{y}_j}^{\alpha^{(u)}}$ at $\alpha^{(u)}$. For all $\alpha_k \geq \alpha^{(u)}$, compute $(\widetilde{\boldsymbol{Y}}_j)_{\alpha_k}$ at each time step $j = 1, \ldots, m$ using $(\widetilde{\boldsymbol{Y}}_j)_{\alpha_k} = \boldsymbol{T}_{\boldsymbol{y}_j}^{\alpha^{(u)}}((\widetilde{\boldsymbol{Y}}_0)_{\alpha_k}, (\widetilde{\boldsymbol{\Theta}})_{\alpha_k})$. Determine $A^{(u)}$.
3. If $R_{\mathrm{A}}^{(u)} = (A^{(u-1)} - A^{(u)})/A^{(u-1)} < \epsilon$, stop. Otherwise, set $\alpha^{(u+1)} = \alpha^{(u)} + \alpha^*(1 - \alpha^{(u)})$ and return to Step 2 with $u = u + 1$.

Note that in Step 2 the new Taylor model at $\alpha^{(u)}$ can only be used to compute state possibility intervals for $\alpha_k \geq \alpha^{(u)}$, for reasons explained in Section 4.2.3. For $\alpha_k < \alpha^{(u)}$, the previously computed values of the possibility intervals remain valid and are unchanged in Step 2.

The procedure outlined above was applied to this problem using $\alpha^* = 0.2$, with iteration-by-iteration results shown in Table 3. If a tolerance of $\epsilon = 0.01$ were used, the iteration would stop after evaluation of three Taylor models ($u = 3$). Fuzzy trajectories (for biomass and substrate only) for this case are shown in Fig. 11, with results at $t = 5.6$ h highlighted. The Area Ratio (relative to use of 100 Taylor models) is 1.0176 (note that in normal use of the iterative procedure one will not know this ratio, since the case of 100 Taylor models is never done). If a tolerance of $\epsilon = 0.001$ were used, the iteration would stop after evaluation of six Taylor models ($u = 6$). Now the Area Ratio is 1.0086. Use of Method 3, with the procedure suggested here, reduces computation time by over an order of magnitude compared to Method 2, with only a very small overestimation of the state membership functions.

6 Concluding Remarks

Numerical models of nonlinear phenomena often incorporate uncertain parameters and initial conditions. If this uncertainty arises from lack of knowledge, not from randomness, then it may appropriate to represent the uncertainty using fuzzy sets or fuzzy numbers. The resulting fuzzy trajectories represent the propagation of this uncertainty throughout the evolution of such nonlinear dynamic systems. We have presented here a new, rigorous approach for computing the fuzzy state trajectories. Current methods for addressing this problem rely on sampling and may underestimate the true effect of uncertainties. Our approach is fundamentally different from current methods. Since it is not based on sampling, it provides mathematically and computationally rigorous results. Variations of the approach allow one to trade-off computational expense and degree of overestimation, but in all cases, rigorous enclosures of the state membership functions are obtained.

Acknowledgements

This work was supported in part by the University of Notre Dame Center for Applied Mathe-

matics. Computational resources were provided in part by the University of Notre Dame Center for Research Computing.

References

Andujar, J. M. & Bravo, J. M. (2005). Multivariable fuzzy control applied to the physical-chemical treatment facility of a cellulose factory. *Fuzzy Sets and Systems*, *150*, 475–492.

Anile, A. M., Deodato, S., & Privetera, G. (1995). Implementing fuzzy arithmetic. *Fuzzy Sets and Systems*, *72*, 239–250.

Arva, P. & Csukas, B. (1987). Fuzzy valued relational algebrae in chemical-engineering. *Hungarian Journal of Industrial Chemistry*, *15*, 1–8.

Berz, M. & Makino, K. (1998). Verified integration of ODEs and flows using differential algebraic methods on high-order Taylor models. *Reliable Computing*, *4*, 361–369.

Chang, P.-T. & Hung, K.-C. (2006). α-cut fuzzy arithmetic: Simplifying rules and a fuzzy function optimization with a decision variable. *IEEE Transactions on Fuzzy Systems*, *14*, 496–510.

Chen, J. Y. & Chang, C. T. (2006). Fuzzy diagnosis method for control systems with coupled feed forward and feedback loops. *Chemical Engineering Science*, *61*, 3105–3128.

Chen, W. C., Chang, N. B., & Shieh, W. K. (2001). Advanced hybrid fuzzy-neural controller for industrial wastewater treatment. *Journal of Environmental Engineering*, *127*, 1048–1059.

Claudel, S., Fonteix, C., Leclerc, J. P., & Lintz, H. G. (2003). Application of the possibility theory to the compartment modelling of flow pattern in industrial processes. *Chemical Engineering Science*, *58*, 4005–4016.

Dohnal, M., Exall, D. I., Carsky, M., Morris, R. M., & Dohnalova, J. (1994). A revitalization of chemical-engineering knowledge with fuzzy calculus. *The Chemical Engineering Journal*, *54*, 155–166.

Dong, W. M. & Shah, H. C. (1987). Vertex method for computing functions of fuzzy variables. *Fuzzy Sets and Systems*, *24*, 65–78.

Dubois, D., Foulloy, L., Mauris, G., & Prade, H. (2004). Probability-possibility transformations, triangular fuzzy sets, and probabilistic inequalities. *Reliable Computing*, *10*, 273–297.

Dubois, D. & Prade, H. (1978). Operations on fuzzy numbers. *International Journal of Systems Science*, *9*, 613–626.

Dubois, D. & Prade, H. (1979). Fuzzy real algebra: Some results. *Fuzzy Sets and Systems*, *2*, 327–348.

Dubois, D. & Prade, H. (1980). *Fuzzy Sets and Systems: Theory and Applications*. New York: Academic Press.

Dubois, D. & Prade, H. (1982). On several representations of an uncertain body of evidence. In M. M. Gupta & E. Sanchez, eds., *Fuzzy Information and Decision Processes*, pp. 167–181, Amsterdam: North-Holland.

Ferson, S. (2002). *RAMAS Risk Calc 4.0 Software: Risk Assessment with Uncertain Numbers*. Boca Raton, FL: Lewis Publishers.

Ferson, S., Ginzburg, L., & Akçakaya, R. (1996). Whereof one cannot speak: When input distributions are unknown. Technical report, Applied Biomathematics, Setauket, NY, available at www.ramas.com/whereof.pdf.

Gromov, Y. Y., Kafarov, V. V., & Matveikin, V. G. (1995). Theory of fuzzy sets in control of chemical engineering processes. *Theoretical Foundations of Chemical Engineering*, *29*, 503–507.

Gromov, Y. Y., Kafarov, V. V., & Matveikin, V. G. (1996). Mathematical modeling of chemical-engineering units under uncertainty. *Theoretical Foundations of Chemical Engineering*, *30*, 75–80.

Guimarães, A. C. F. & Lapa, C. M. F. (2004). Fuzzy FMEA applied to PWR chemical and volume control system. *Progress in Nuclear Energy*, *44*, 191–213.

Gupta, C. P. (1993). A note on the transformation of possibilistic information into probabilistic information for investment decisions. *Fuzzy Sets and Systems*, *56*, 175–182.

Hanratty, P. J. & Joseph, B. (1992). Decision making in chemical engineering and expert systems – Application of the analytic hierarchy process to reactor selection. *Computers & Chemical Engineering*, *16*, 849–860.

Hanratty, P. J., Joseph, B., & Dudukovic, M. P. (1992). Knowledge representation and reasoning

in the presence of uncertainty in an expert system for laboratory reactor selection. *Industrial & Engineering Chemistry Research*, *31*, 228–238.

Hansen, E. R. & Walster, G. W. (2004). *Global Optimization Using Interval Analysis*. 2nd ed., New York: Marcel Dekker.

Hanss, M. (2002). The transformation method for the simulation and analysis of systems with uncertain parameters. *Fuzzy Sets and Systems*, *130*, 277–289.

Hanss, M. (2005). *Applied Fuzzy Arithmetic: An Introduction With Engineering Applications*. Berlin: Springer-Verlag.

Hassana, C. R. C., Balasubramaniam, P. A. L., Raman, A. A. A., Mahmood, N. Z., Hung, F. C., & Sulaiman, N. M. N. (2009). Inclusion of human errors assessment in failure frequency analysis–a case study for the transportation of ammonia by rail in Malaysia. *Process Safety Progress*, *28*, 60–67.

Henson, M. A. & Seborg, D. E. (1997). Feedback linearizing control. In M. A. Henson & D. E. Seborg, eds., *Nonlinear Process Control*, pp. 149–231, Upper Saddle River, NJ: Prentice-Hall.

Jaulin, L., Kieffer, M., Didrit, O., & Walter, É. (2001). *Applied Interval Analysis*. London: Springer-Verlag.

Johansen, T. A. & Foss, B. A. (1997). Operating regime based process modeling and identification. *Computers & Chemical Engineering*, *21*, 159–176.

Kaucsár, M., Axente, D., Cosma, V., & Baldea, A. (2007). Fuzzy logic used to control a n-15 isotope separation plant. *Revista de Chimie*, *58*, 809–815.

Kaufmann, A. & Gupta, M. M. (1985). *Introduction to Fuzzy Arithmetic: Theory and Applications*. New York: Van Nostrand Reinhold Co.

Kearfott, R. B. (1996). *Rigorous Global Search: Continuous Problems*. Dordrecht, The Netherlands: Kluwer Academic Publishers.

Klir, G. J. & Parviz, B. (1992). Probability-possibility transformations: A comparison. *International Journal of General Systems*, *21*, 291–310.

Kosheleva, O., Cabrera, S. D., Gibson, G. A., & Koshelev, M. (1997). Fast implementations of fuzzy arithmetic operations using fast fourier transform (FFT). *Fuzzy Sets and Systems*, *91*, 269–277.

Li, W. Y. & Hyman, J. M. (2004). Computer arithmetic for probability distribution variables. *Reliability Engineering & System Safety*, *85*, 191–209.

Lin, Y. & Stadtherr, M. A. (2007). Validated solutions of initial value problems for parametric ODEs. *Applied Numerical Mathematics*, *57*, 1145–1162.

Makino, K. & Berz, M. (1996). Remainder differential algebras and their applications. In M. Berz, C. Bishof, G. Corliss, & A. Griewank, eds., *Computational Differentiation: Techniques, Applications, and Tools*, pp. 63–74, Philadelphia, PA: SIAM.

Makino, K. & Berz, M. (1999). Efficient control of the dependency problem based on Taylor model methods. *Reliable Computing*, *5*, 3–12.

Makino, K. & Berz, M. (2003). Taylor models and other validated functional inclusion methods. *International Journal of Pure and Applied Mathematics*, *4*, 379–456.

Makino, K. & Berz, M. (2004). Taylor model range bounding schemes. Presented at Third International Workshop on Taylor Methods, Miami Beach, FL, USA, see http://bt.pa.msu.edu/TM/Miami2004/TM-Slides/Miami-GO04.pdf.

Makino, K. & Berz, M. (2005). Verified global optimization with Taylor model-based range bounders. *Transactions on Computers*, *11*, 1611–1618.

Meel, A. & Seider, W. D. (2006). Plant-specific dynamic failure assessment using Bayesian theory. *Chemical Engineering Science*, *61*, 7036–7056.

Moore, R. E., Kearfott, R. B., & Cloud, M. J. (2009). *Introduction to Interval Analysis*. Philadelphia, PA: SIAM Press.

Nahmias, S. (1977). Fuzzy variables. *Fuzzy Sets and Systems*, *1*, 97–110.

Nedialkov, N. S. (1999). *Computing Rigorous Bounds on the Solution of an Initial Value Problem for an Ordinary Differential Equation*. Ph.D. thesis, University of Toronto.

Nedialkov, N. S., Jackson, K. R., & Pryce, J. D. (2001). An effective high-order interval method for validating existence and uniqueness of the solution of an IVP for an ODE. *Reliable Computing*, *7*, 449–465.

Neher, M., Jackson, K. R., & Nedialkov, N. S. (2007). On Taylor model based integration of ODEs. *SIAM Journal on Numerical Analysis*, *45*, 236–262.

Neumaier, A. (1990). *Interval Methods for Systems of Equations*. Cambridge, UK: Cambridge University Press.

Neumaier, A. (2003). Taylor forms – Use and limits. *Reliable Computing*, *9*, 43–79.

Otto, K. N., Lewis, A. D., & Antonsson, E. K. (1993). Approximating α-cuts with the vertex method. *Fuzzy Sets and Systems*, *55*, 43–50.

Rauh, A., Brill, M., & Günther, C. (2009). A novel interval arithmetic approach for solving differential-algebraic equations with ValEncIA-IVP. *International Journal of Applied Mathematics and Computer Science*, *19*, 381–397.

Sahlodin, A. M. & Chachuat, B. (2011a). Convex/concave relaxations of parametric ODEs using Taylor models. *Computers & Chemical Engineering*, *35*, 844–857.

Sahlodin, A. M. & Chachuat, B. (2011b). Discretize-then-relax approach for convex/concave relaxations of the solutions of parametric ODEs. *Applied Numerical Mathematics*, *61*, 803–820.

Sanjuan, M., Kandel, A., & Smith, C. A. (2006). Design and implementation of a fuzzy supervisor for on-line compensation of nonlinearities: An instability avoidance module. *Engineering Applications of Artificial Intelligence*, *19*, 323–333.

Schmitz, G. P. J. & Aldrich, C. (1998). Neurofuzzy modeling of chemical process systems with ellipsoidal radial basis function neural networks and genetic algorithms. *Computers & Chemical Engineering*, *22*, S1001–S1004.

Seng, K.-Y., Nestorov, I., & Vicini, P. (2007). Simulating pharmacokinetic and pharmacodynamic fuzzy-parameterized models: a comparison of numerical methods. *Journal of Pharmacokinetics and Pharmacodynamics*, *34*, 595–621.

Stephane, N. & Marc, L. L. J. (2008). Case-based reasoning for chemical engineering design. *Chemical Engineering Research and Design*, *86*, 648–658.

Takeda, K., Shibata, B. Y., Tsuge, Y., & Matsuyama, H. (1994). Robust fault diagnosis for the chemical plant based on the qualitative model. *Kagaku Kogaku Ronbunshu*, *20*, 373–381.

Tsekouras, G., Sarimveis, H., Raptis, C., & Bafas, G. (2002). A fuzzy logic approach for the classification of product qualitative characteristics. *Computers & Chemical Engineering*, *26*, 429–438.

Vrba, J. (1991). FUSIM – a program for fuzzy linguistic modeling and simulation of technological processes. *Systems Analysis Modelling Simulation*, *8*, 115–137.

Williamson, R. C. & Downs, T. (1990). Probabilistic arithmetic I. Numerical methods for calculating convolutions and dependency bounds. *International Journal of Approximate Reasoning*, *4*, 89–158.

Wood, K. L., Otto, K. N., & Antonsson, E. K. (1992). Engineering design calculations with fuzzy parameters. *Fuzzy Sets and Systems*, *52*, 1–20.

Yang, H. Q., Yao, H., & Jones, J. D. (1993). Calculating functions of fuzzy numbers. *Fuzzy Sets and Systems*, *55*, 273–283.

Yong, M., Zheng, X., Zheng, Y., Youxian, S., & Zheng, W. (2007). Fault diagnosis based on fuzzy support vector machine with parameter tuning and feature selection. *Chinese Journal of Chemical Engineering*, *15*, 233–239.

Yu, C. C. & Lee, C. (1991). Fault diagnosis based on qualitative quantitative process knowledge. *AIChE Journal*, *37*, 617–628.

Zadeh, L. A. (1965). Fuzzy sets. *Information and Control*, *8*, 338–353.

Zadeh, L. A. (1975a). The concept of a linguistic variable and its application to approximate reasoning—Part I. *Information Sciences*, *8*, 199–249.

Zadeh, L. A. (1975b). The concept of a linguistic variable and its application to approximate reasoning—Part II. *Information Sciences*, *8*, 301–357.

Zadeh, L. A. (1975c). The concept of a linguistic variable and its application to approximate reasoning—Part III. *Information Sciences*, *9*, 43–80.

Zadeh, L. A. (1978). Fuzzy sets as a basis for a theory of possibility. *Fuzzy Sets and Systems*, *1*, 3–28.

Zhang, S. L., Ye, B. C., Chu, J., Zhuang, Y. P., & Guo, M. J. (2006). From multi-scale methodology to systems biology: To integrate strain improvement and fermentation optimization. *Journal of Chemical Technology and Biotechnology*, *81*, 734–745.

Table 1: Tradeoff between bound tightness and CPU time in comparing Methods 2 and 3 in Example 3 (two-state bioreactor models). For Method 2, the Area Ratio and Maximum Interval Ratio are one by definition

Kinetic Model	Quantity	Method Used	Number of TMs	CPU Time (s)	Area Ratio	Maximum Interval Ratio
Monod	$X(20)$	2	100	110	1	1
		3	1	1	1.0004	1.0010
	$S(20)$	2	100	100	1	1
		3	1	1	1.0002	1.0004
Haldane	$X(20)$	2	100	110	1	1
		3	1	1	1.0010	1.0032
	$S(20)$	2	100	100	1	1
		3	1	1	1.0013	1.0039

Table 2: Tradeoff between bound tightness and CPU time in comparing Methods 2 and 3, and effect of α-level for second Taylor model (reset level) in Method 3, for Example 4 (three-state bioreactor model). The Area Ratio and Maximum Interval Ratio are based on an average over all three state variables at $t = 16$ h.

Method Used	Number of Taylor Models	α Value(s)	CPU Time (s)	Area Ratio	Maximum Interval Ratio
2	100	—	785	1	1
3	1	0.01	8	1.0724	1.1976
3	2	0.01, 0.10	15	1.0382	1.1182
		0.01, 0.20	15	1.0244	1.0723
		0.01, 0.30	15	1.0297	1.0702
		0.01, 0.40	15	1.0271	1.0668
		0.01, 0.50	15	1.0306	1.0828
		0.01, 0.60	15	1.0370	1.0981
		0.01, 0.70	15	1.0449	1.1147
		0.01, 0.80	15	1.0535	1.1345
		0.01, 0.90	15	1.0626	1.1595

Table 3: Results from algorithm for applying Method 3. The relative area difference is based on $t = 16$ h.

Number of Taylor Models (u)	α Value(s)	CPU Time (s)	Relative Area Difference ($R_{\mathrm{A}}^{(u)}$)
1	0.01	8	—
2	0.01, 0.20	15	0.0448
3	0.01, 0.20, 0.36	24	0.00664
4	0.01, 0.20, 0.36, 0.49	33	0.00609
5	0.01, 0.20, 0.36, 0.49, 0.59	41	0.00198
6	0.01, 0.20, 0.36, 0.49, 0.59, 0.67	48	0.00079

List of Figure Captions

Figure 1: A generic fuzzy number $\widetilde{A}$ with membership function $\mu_{\widetilde{A}}$, showing its support and core intervals, and an arbitrary α-cut interval $(\widetilde{A})_\alpha$.

Figure 2: Different types of fuzzy numbers.

Figure 3: Stepped fuzzy number resulting from expert survey example in text.

Figure 4: Addition of fuzzy numbers, $\widetilde{A} + \widetilde{B} = \widetilde{C}$.

Figure 5: Fuzzy number inputs for the Lotka-Volterra competition model (Example 1): (a) Membership function for $r_2 = \theta_1$; (b) Membership function for $a_{21} = \theta_2$.

Figure 6: VSPODE enclosures and fuzzy trajectories for Example 1 (fuzzy states at 40 days highlighted): (a) Species 1; (b) Species 2.

Figure 7: VSPODE enclosures and fuzzy trajectories for Example 2 (fuzzy states at 22.2 days highlighted): (a) Prey species; (b) Predator species.

Figure 8: Fuzzy number inputs for the Monod bioreactor model (Example 3): (a) Membership function for D; (b) Membership function for K_S.

Figure 9: VSPODE enclosures and fuzzy trajectories for Example 3 with Monod kinetics (states at 8.0 h highlighted): (a) Biomass concentration; (b) Substrate concentration.

Figure 10: VSPODE enclosures and fuzzy trajectories for Example 3 with Haldane kinetics (states at 11.2 h highlighted): (a) Biomass concentration; (b) Substrate concentration.

Figure 11: VSPODE enclosures and fuzzy trajectories for Example 4 (states at 5.6 h highlighted):

(a) Biomass concentration; (b) Substrate concentration.

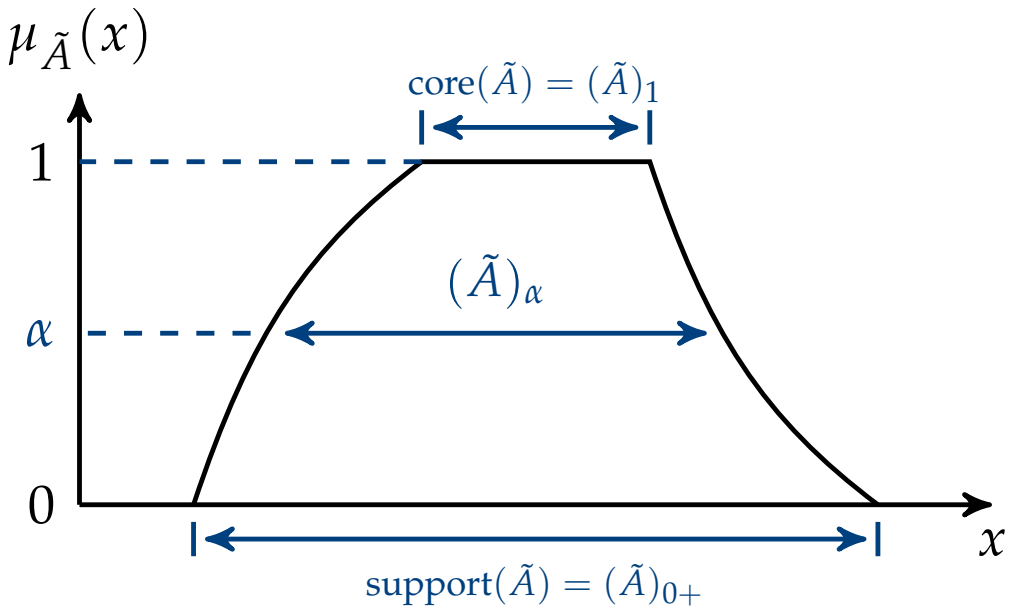

Figure 1: A generic fuzzy number $\widetilde{A}$ with membership function $\mu_{\widetilde{A}}$, showing its support and core intervals, and an arbitrary α-cut interval $(\widetilde{A})_\alpha$.

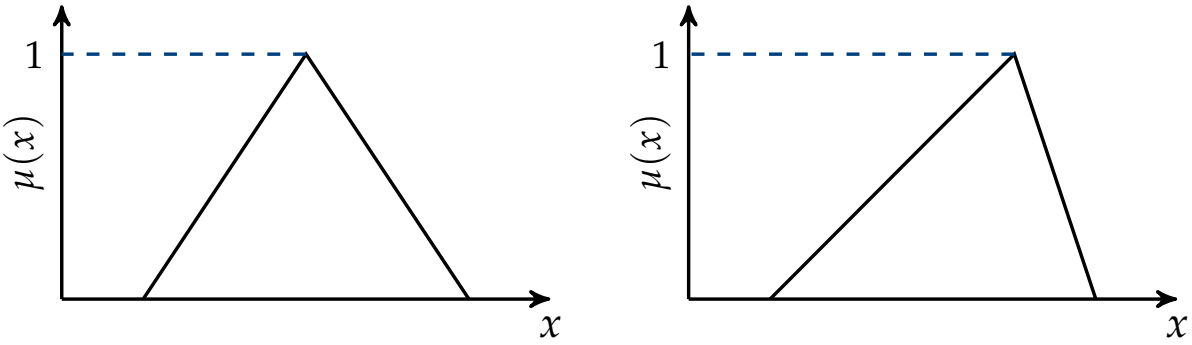

(a) A triangular fuzzy number (symmetric)

(b) A triangular fuzzy number (asymmetric)

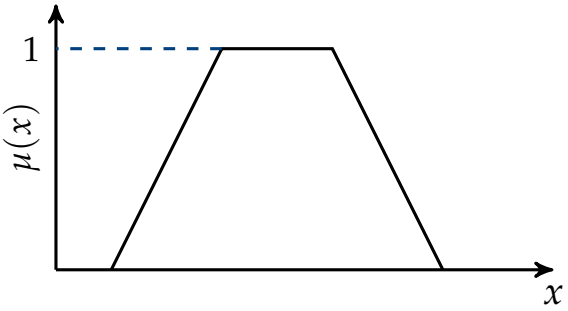

(c) A trapezoidal fuzzy number

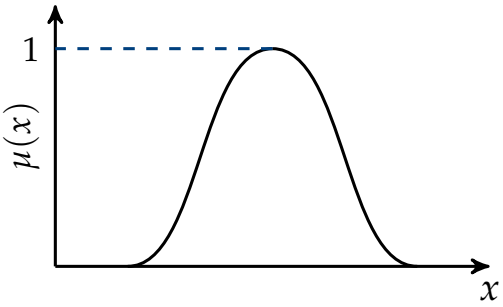

(d) A Gaussian fuzzy number

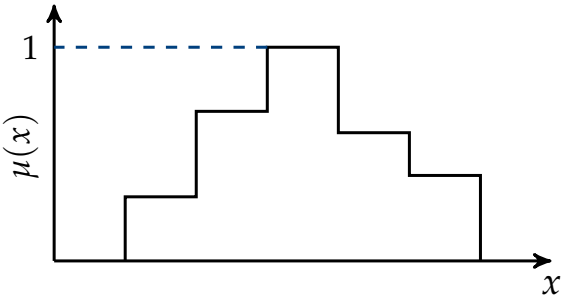

(e) A stepped (discrete) fuzzy number

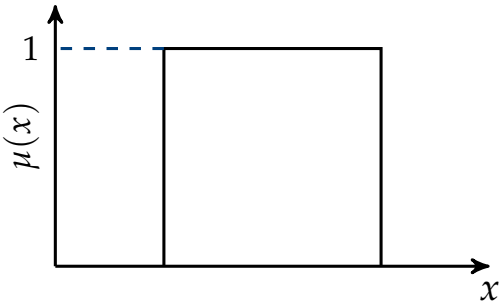

(f) An interval

Figure 2: Different types of fuzzy numbers.

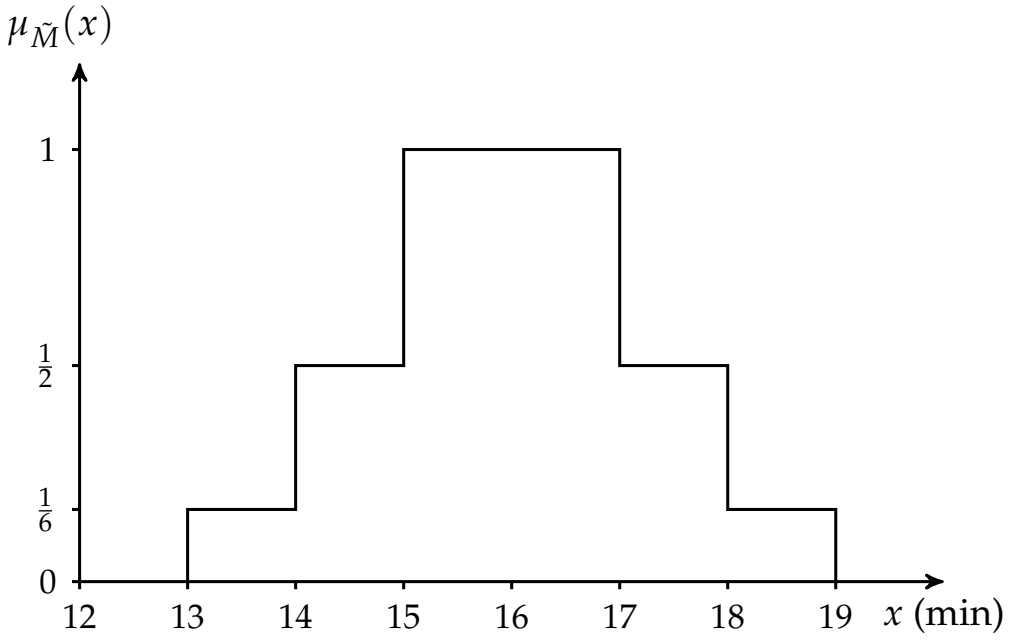

Figure 3: Stepped fuzzy number resulting from expert survey example in text.

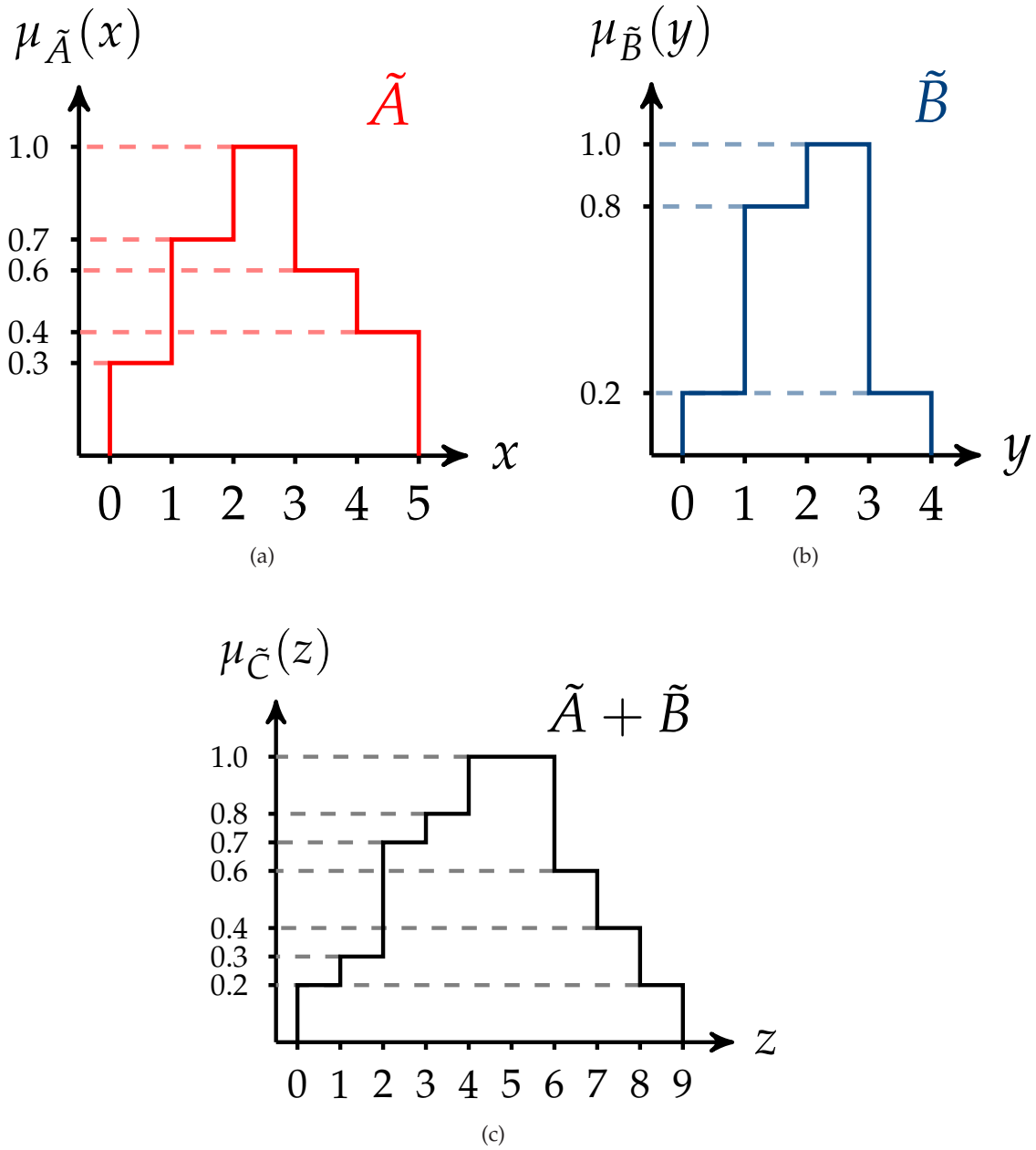

Figure 4: Addition of fuzzy numbers, $\widetilde{A} + \widetilde{B} = \widetilde{C}$.

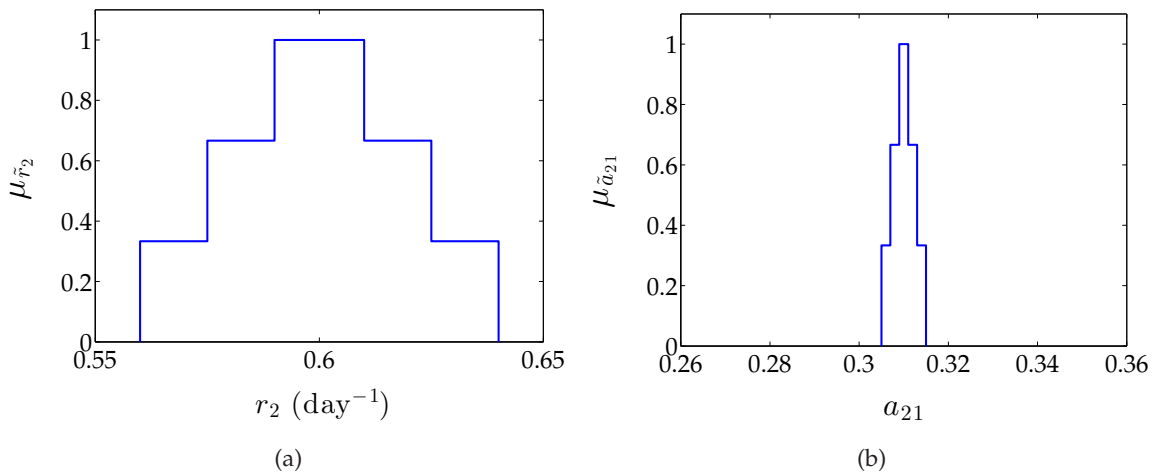

Figure 5: Fuzzy number inputs for the Lotka-Volterra competition model (Example 1): (a) Membership function for $r_2 = \theta_1$; (b) Membership function for $a_{21} = \theta_2$.

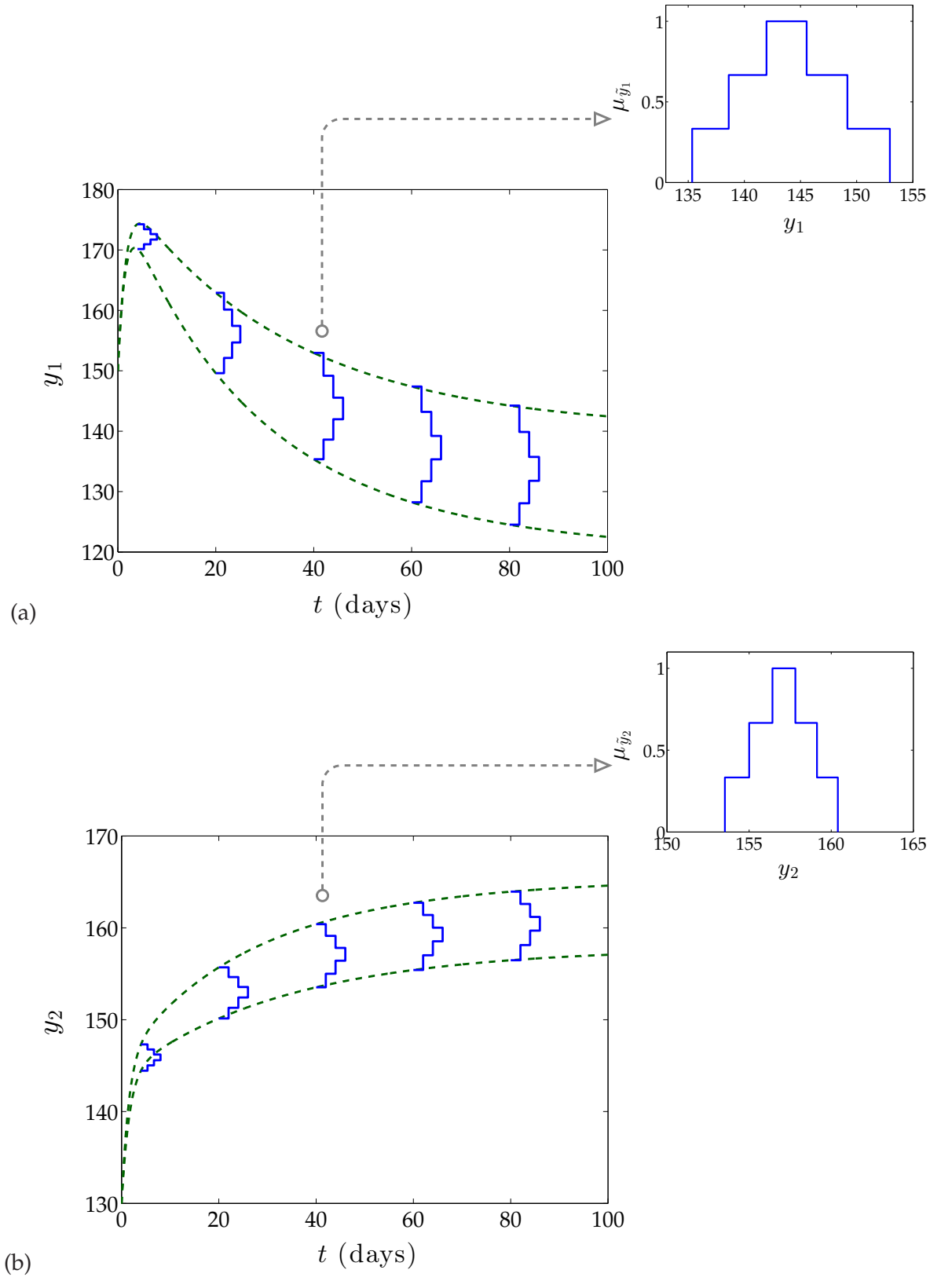

Figure 6: VSPODE enclosures and fuzzy trajectories for Example 1 (fuzzy states at 40 days highlighted): (a) Species 1; (b) Species 2.

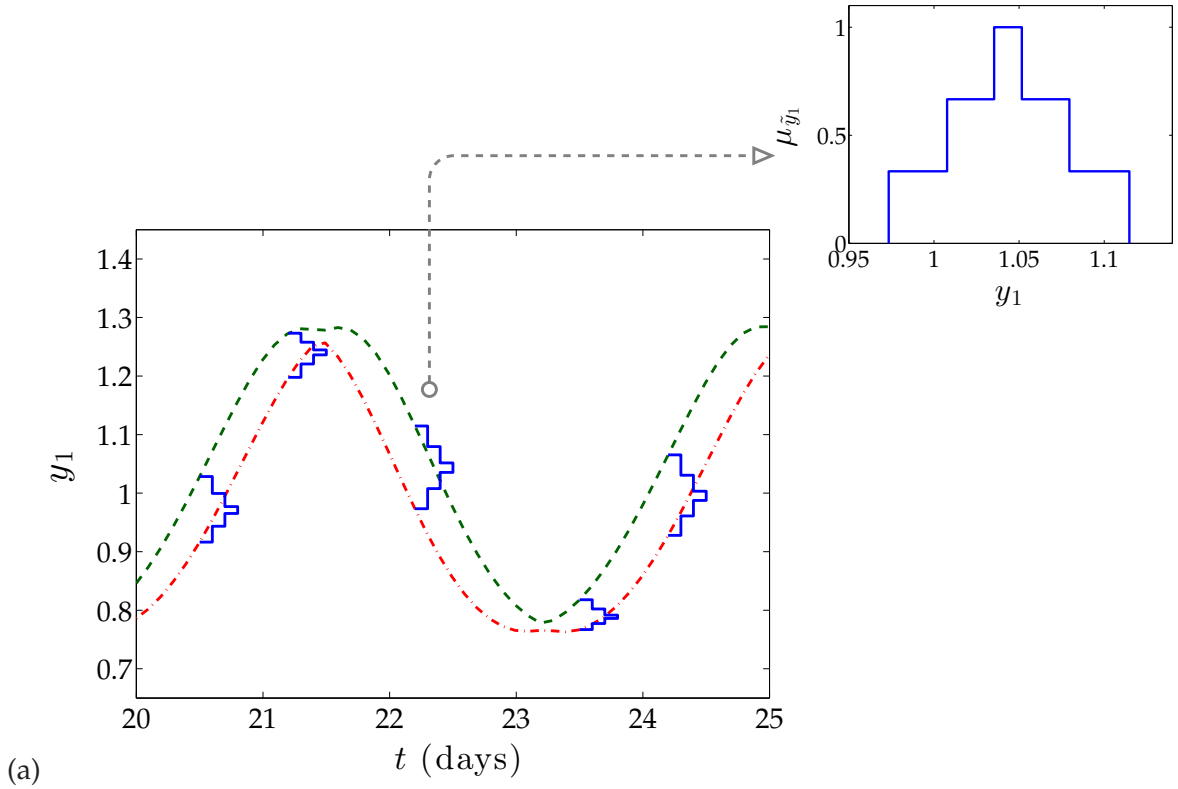

(a)

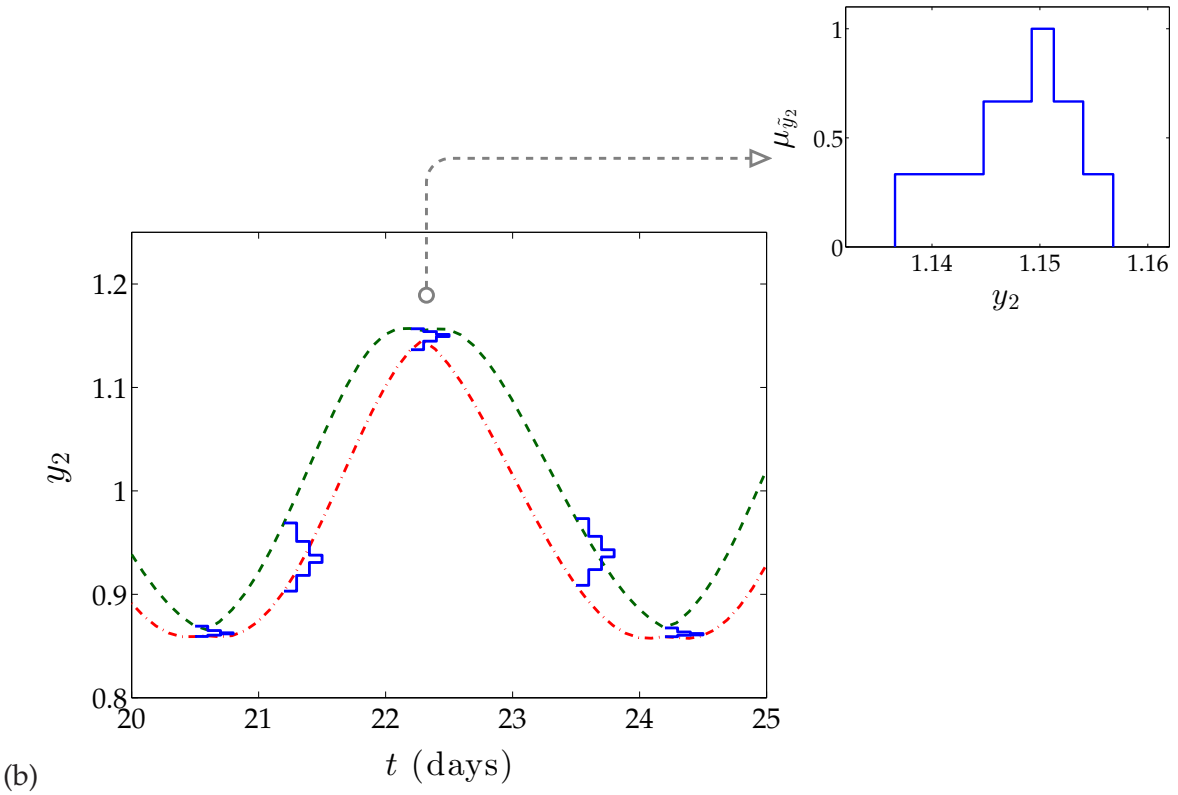

(b)

Figure 7: VSPODE enclosures and fuzzy trajectories for Example 2 (fuzzy states at 22.2 days highlighted): (a) Prey species; (b) Predator species.

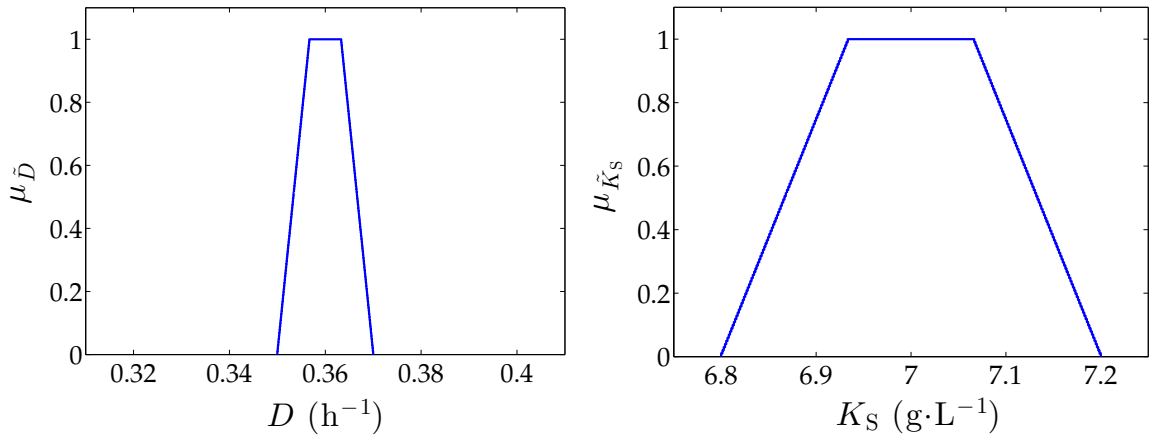

Figure 8: Fuzzy number inputs for the Monod bioreactor model (Example 3): (a) Membership function for D; (b) Membership function for K_S.

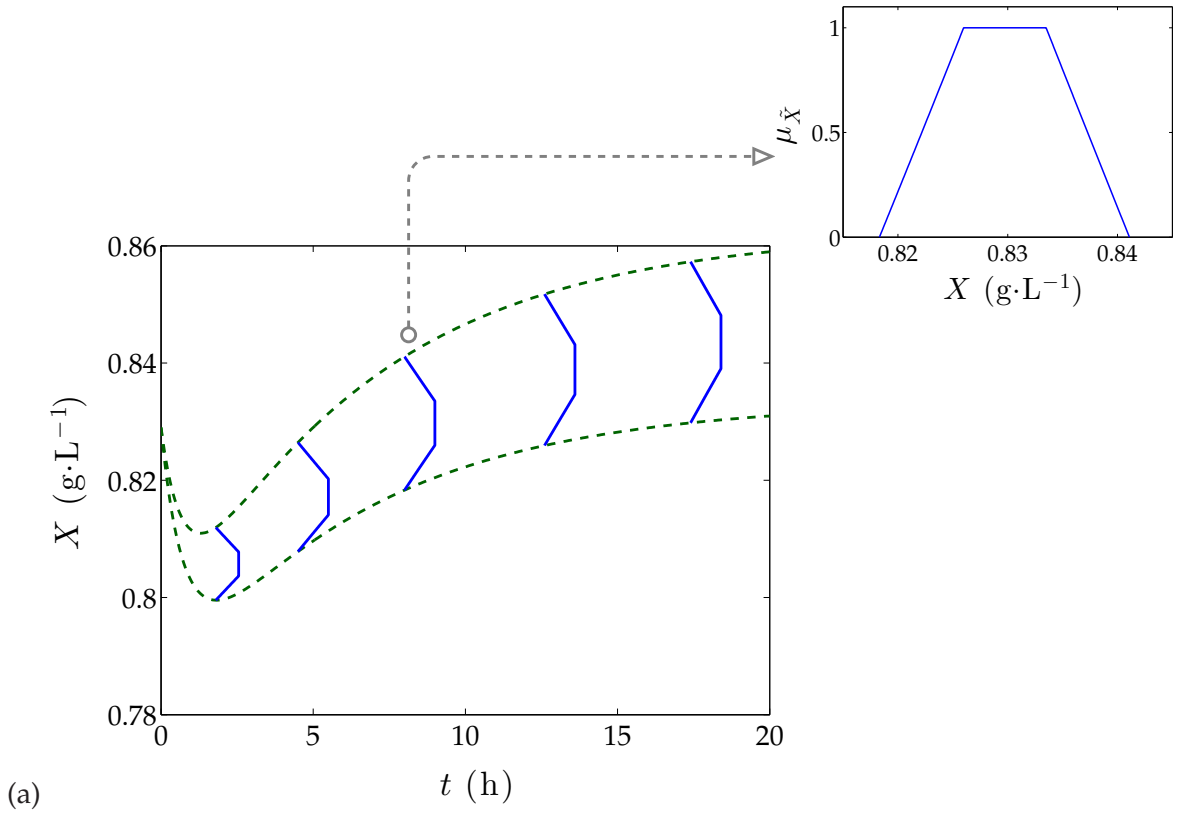

(a)

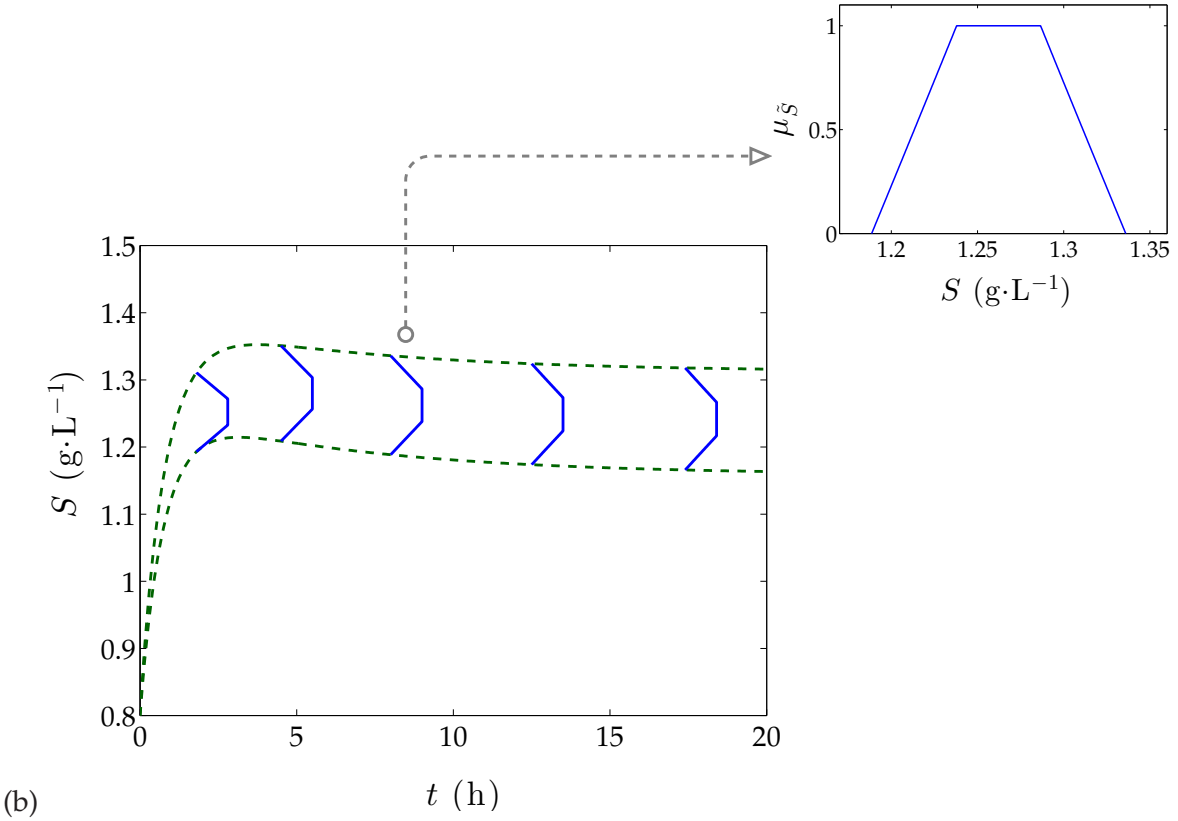

(b)

Figure 9: VSPODE enclosures and fuzzy trajectories for Example 3 with Monod kinetics (states at 8.0 h highlighted): (a) Biomass concentration; (b) Substrate concentration.

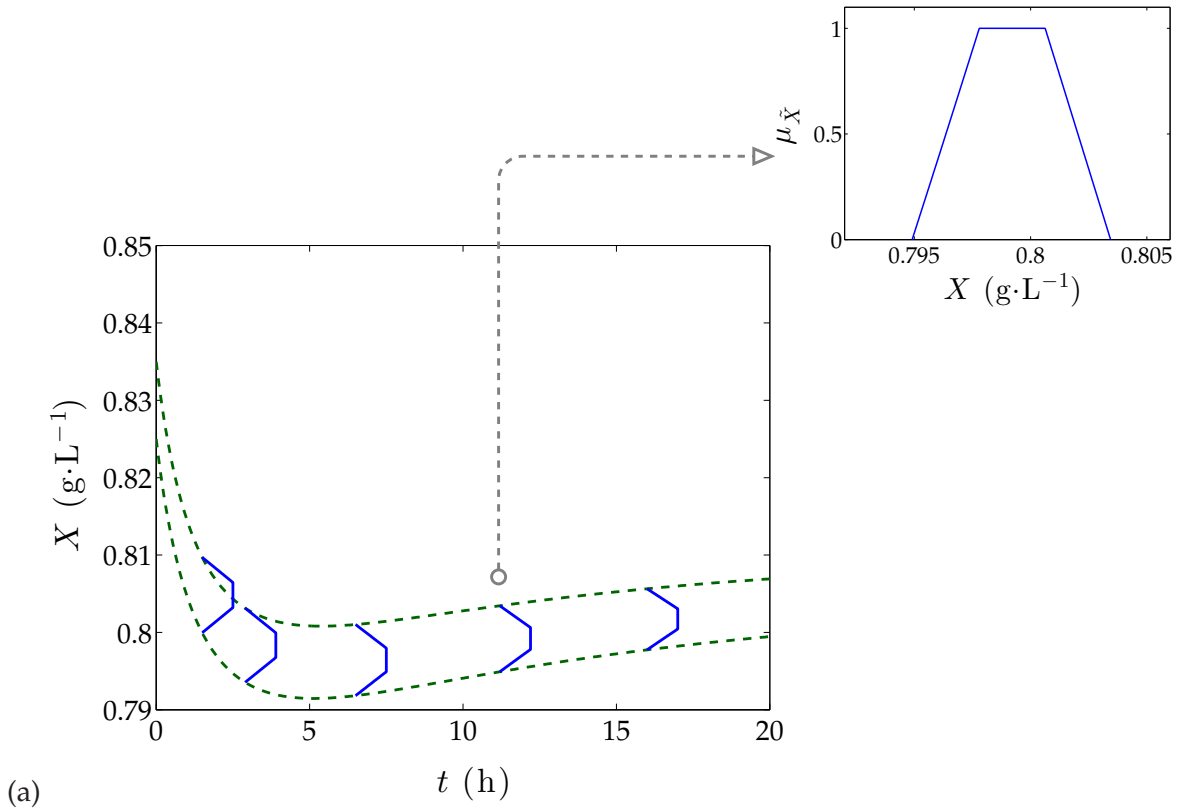

(a)

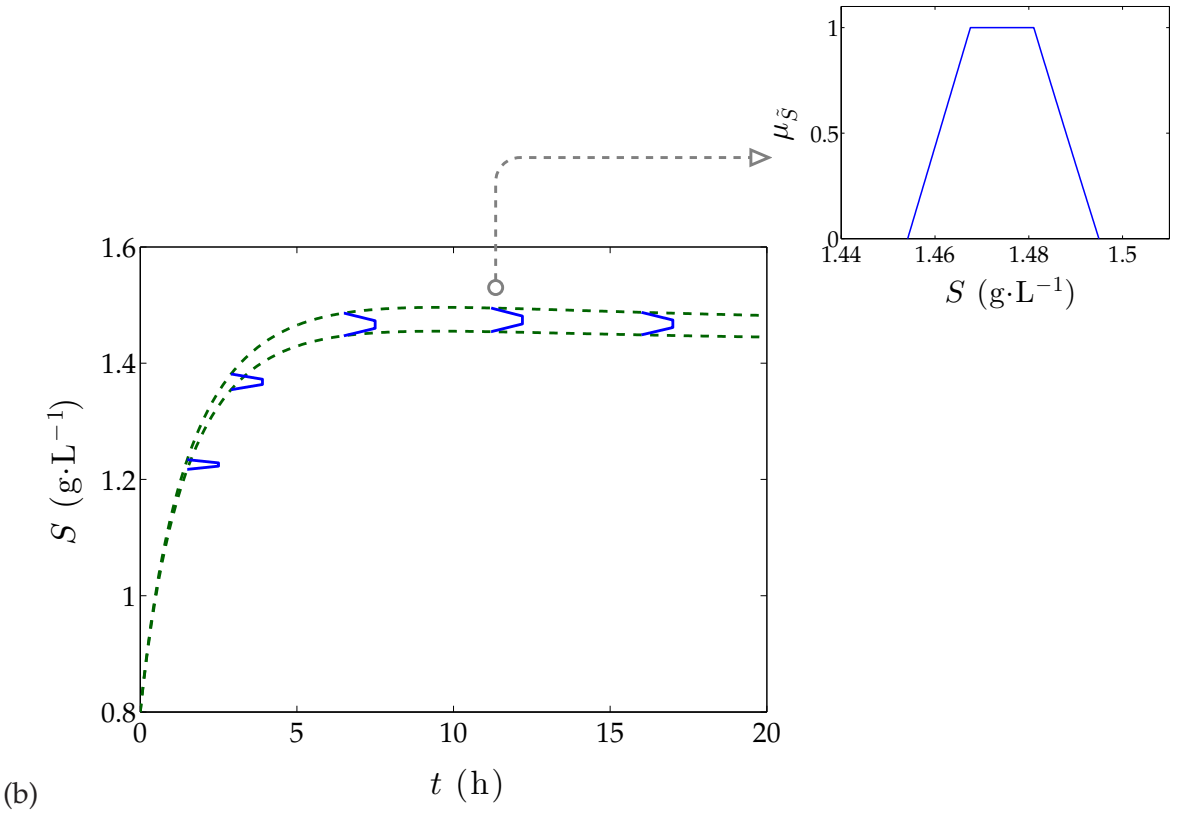

(b)

Figure 10: VSPODE enclosures and fuzzy trajectories for Example 3 with Haldane kinetics (states at 11.2 h highlighted): (a) Biomass concentration; (b) Substrate concentration.

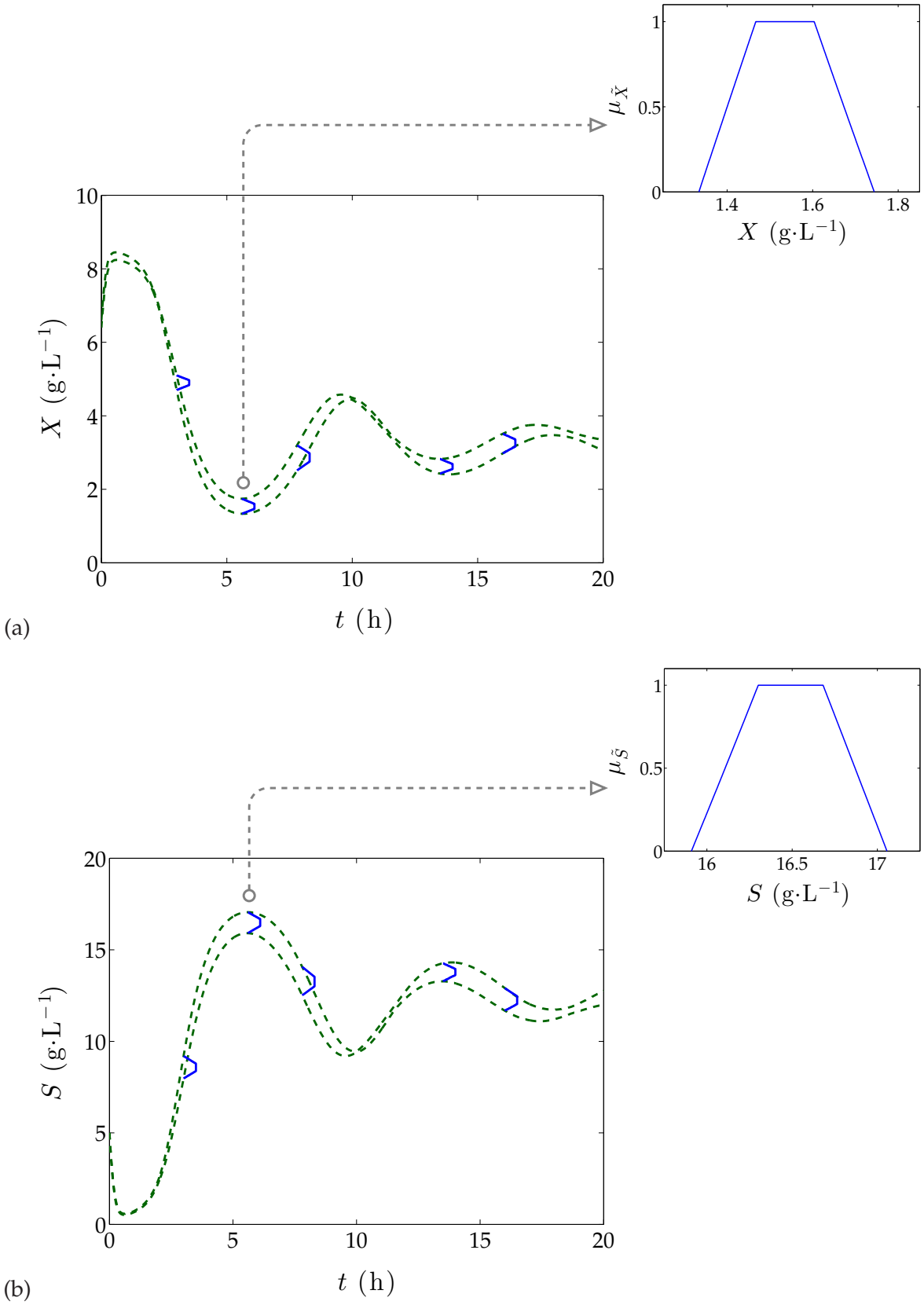

Figure 11: VSPODE enclosures and fuzzy trajectories for Example 4 (states at 5.6 h highlighted): (a) Biomass concentration; (b) Substrate concentration.